Pharmacological Research 227 (2026) 108187

Contents lists available at ScienceDirect

Pharmacological Research

journal homepage: www.elsevier.com/locate/yphrs

Bruton protein-tyrosine kinase (BTK) FDA-approved small molecule inhibitors used for the management of neoplastic and inflammatory disorders

Robert Roskoski Jr

Blue Ridge Institute for Medical Research, 221 Haywood Knolls Drive, Hendersonville, NC 28791, United States

ARTICLE INFO

Keywords:
Chronic immune disease
Chronic lymphocytic leukemia
Follicular lymphoma
Mantle cell lymphoma
Marginal zone lymphoma
Waldenström macroglobulinemia

Chemical compounds studied in this article:
Acalabrutinib (PubMed CID: 71226662)
Cyclophosphamide (PubMed CID: 2907)
Ibrutinib (PubMed CID: 24821094)
Imatinib (PubMed CID: 5291)
Oncovin/vincristine (PubMed CID: 5388992)
Prednisone (PubMed CID: 5865)
Pirtobrutinib (PubMed CID: 129269915)
Remibrutinib (PubMed CID: 118107483)
Rilzabrutinib (PubMed CID: 73388818)
Zanubrutinib (PubMed CID: 135565884)

ABSTRACT

The Bruton nonreceptor protein-tyrosine kinase (BTK) plays a central role in B cell antigen receptor signaling. Following B cell receptor activation, the Src protein kinase Lyn and the spleen protein kinase (Syk) activate BTK. It then mediates the phosphorylation and activation of phospholipase Cγ2 (PLCγ2). The Ras/RAF/MEK/ERK and NF-κB pathways are downstream of PLCγ2. These signaling modules participate in the affinity maturation of antibody-producing B cells by somatic hypermutation. The absence of BTK results in X-linked agammaglobulinemia. BTK contains an amino-terminal PH (pleckstrin homology) domain that interacts with phosphatidyl inositol trisphosphate within the plasma membrane to promote its membrane association. This is followed by a TEC homology segment, an SH3 and SH2 domain, and finally a carboxyterminal protein kinase domain. Aberrant B cell receptor signaling occurs in several B cell neoplasms including follicular lymphoma (treated with zanubrutinib, a BTK inhibitor), mantle cell lymphoma (acalabrutinib, pirtobrutinib, zanubrutinib), marginal zone lymphoma (zanubrutinib), chronic lymphocytic leukemia and small lymphocytic lymphoma (ibrutinib, acalabrutinib, zanubrutinib, pirtobrutinib), and Waldenström macroglobulinemia (ibrutinib, zanubrutinib). Chronic spontaneous urticaria and chronic immune thrombocytopenia are driven by B cell dysfunction. The former is treated with remibrutinib and the latter is treated with rilzabrutinib, both of which inhibit BTK. Four drugs (ibrutinib, acalabrutinib, zanubrutinib, remibrutinib) form an irreversible covalent bond and rilzabrutinib forms a reversible covalent bond with BTK Cys481. Pirtobrutinib fails to form a covalent bond and is a reversible BTK inhibitor. The FDA-approvals of rilzabrutinib and remibrutinib (2025) represent the first nononcologic authorizations for BTK antagonists.

1. Biology of Bruton protein-tyrosine kinase

Ogden Carr Bruton (1908–2003), a pediatrician at Walter Reed Army Hospital in Washington, D.C. reported on the first case of agammaglobulinemia in 1952 [1]. Bruton kinase was initially discovered in 1993 and found to be a nonreceptor protein-tyrosine kinase that is nonfunctional in X-linked agammaglobulinemia (XLA) [2–4]. Immunoglobulins and B lymphocytes are lacking in affected males with this rare condition rendering them susceptible to infections, but they respond beneficially to human immunoglobulin injections [5]. Males with this malady lack significant alterations in cells other than B cells, and this finding is concordant with the limitation of clinical features to B cell immunity.

During development, each B cell joins immunoglobulin variable (V), diversity (D), and junction genes (J) to create a distinctive amino acid

Abbreviations: A, alanine; ALL, acute lymphocytic leukemia; AML, acute myelogenous leukemia; AS, activation segment; CHOP, cyclophosphamide, hydroxydaunorubicin, oncovin (vincristine), prednisone; CLL, chronic lymphocytic leukemia; CS or C-spine, catalytic spine; CL, catalytic loop; COP, cyclophosphamide, oncovin, prednisone; CVP, cyclophosphamide, vincristine, prednisone; DAG, diacylglycerol; DLBCL, diffuse large B cell lymphoma; FCM, fludarabine, cyclophosphamide, mitoxantrone; FL, follicular lymphoma; HD, Hodgkin disease; HΦ or Φ, hydrophobic; IP_3, inositol 1,4,5 trisphosphate; IP_6, inositol 1,2,3,4,5,6 hexakisphosphate; K, lysine; KLIFS-3, kinase-ligand interaction fingerprint and structure residue-3; MCL, mantle cell lymphoma; MDS, myelodysplastic syndrome; MINE, mensa (sodium 2-mercaptoethane sulfonate), ifosfamide, novantrone (mitoxantrone), etoposide; MM, multiple myeloma; MW, molecular weight; MZL, marginal zone lymphoma; NF, nuclear factor; NHL, non-Hodgkin lymphoma; NSCLC, non-small cell lung cancer; PKA/C, protein kinase A or C; PIP_2, phosphatidyl inositol 4,5 bisphosphate; PIP_3, phosphatidyl inositol 3,4,5 trisphosphate; RA, rheumatoid arthritis; R-FC, rituximab, fludarabine, cyclophosphamide; RS or R-spine, regulatory spine; Sh1, shell residue 1; SLL, small lymphocytic lymphoma; WM, Waldenström macroglobulinemia, Y, tyrosine.

E-mail address: rrj@brimr.org.

https://doi.org/10.1016/j.phrs.2026.108187
Received 31 March 2026; Received in revised form 1 April 2026; Accepted 2 April 2026
Available online 3 April 2026

sequence that produces the antigen-binding site of the B cell receptor [6]. B cell receptor action requires a network of adaptors and protein kinases that convert antigenic stimulation into intracellular signaling. The B cell receptor complex is made up of the receptor interacting with a disulfide-linked Igα-Igβ heterodimer. After antigenic activation of the receptor, the Lyn and Src-family kinases catalyze the phosphorylation of tyrosine residue pairs in the Igα-Igβ immunoreceptor tyrosine-based activation motifs (ITAMs) thereby generating a binding site for the two SH2 domains of Syk (spleen tyrosine kinase) [7]. Syk engages and activates PI3 kinase-δ, which mediates the conversion of membrane-bound phosphatidyl inositol 4,5 bisphosphate (PIP_2) to phosphatidyl inositol 3,4,5-trisphosphate (PIP_3). The N-terminal PH lipid-interaction component of BTK is drawn to PIP_3 thereby allowing Syk and Lyn to catalyze the *trans*-phosphorylation of the BTK activation segment at Y551 resulting in enzyme activation. The attraction of BTK dimers to membrane associated PIP_3 molecules also produces activation segment *trans*-autophosphorylation and activation.

BTK mediates the phosphorylation of PLCγ2 at residues Y753 and Y759 to increase phospholipase activity [8]. PLCγ2 mediates the hydrolysis of PIP_2 to yield diacylglycerol (DAG) and inositol trisphosphate (IP_3). IP_3 liberates Ca^{2+} from the intracellular endoplasmic reticulum, which stimulates PLCγ2. In turn, Ca^{2+} and DAG activate PKCβ, which leads to the stimulation of the Ras/RAF/MEK/ERK signaling pathway that promotes cell growth and proliferation [9–15]. PKCβ also stimulates NF-κB using a protein complex that includes caspase recruitment domain-containing protein 11 (CARD11), B cell lymphoma protein 10 (BCL10), and mucosa-associated lymphoid translocation protein 1 (MALT1) (Fig. 1). The inhibitor of kappa Bα (IκBα) neutralizes the NF-κB transcription factor by nullifying its nuclear localization signal and keeping it sequestered in the cytoplasm in an inactive state. The inhibitor of κB kinase (IKK) mediates the phosphorylation of the inhibitory IκBα that promotes its (i) dissociation from NF-κB, (ii) ubiquitylation, and (iii) proteosomal degradation. Free or unsequestered NF-κB is translocated into the nucleus and regulates the expression of approximately 500 genes. It is a swiftly acting transcription factor that regulates, *inter alia*, cytokine production and cell survival. In addition, BTK participates in the important chemokine-mediated homing and adhesion of B cells [16]. Following BTK inhibition, B cells may be liberated from lymphatic tissue into the blood stream, which is commonly observed after treatment with BTK blockers. In addition to its role in B cell antigen-receptor signaling, BTK also contributes to chemokine and Toll-like receptor (TLR) signaling (TLRs are sensors in the innate immune system that recognize structurally conserved molecules derived from microbes and host damaged cells). Moreover, there is a general increase in B cell antigen receptor signaling in various B cell lymphomas.

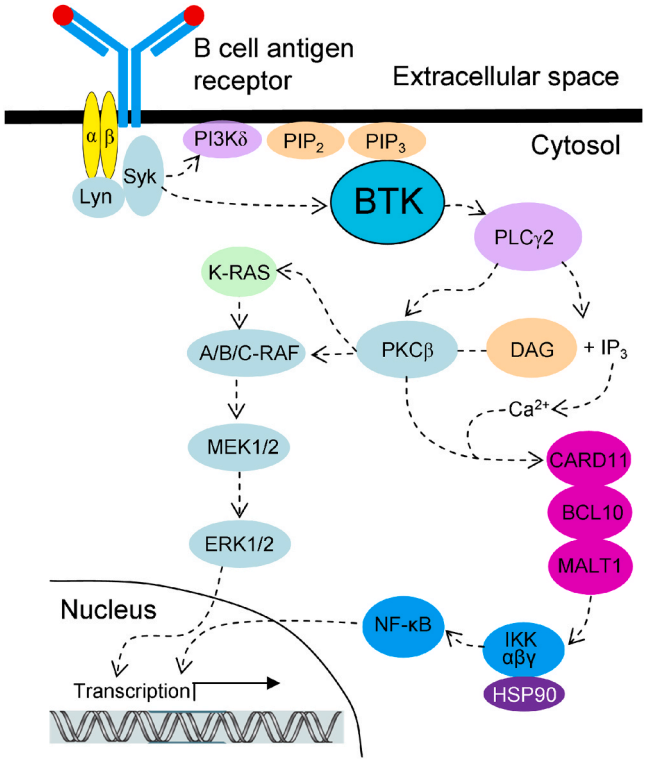

Fig. 1. Role of Bruton protein-tyrosine kinase in B cell receptor signaling. The dashed arrows indicate that several steps may be involved.

2. Biochemistry of Bruton protein-tyrosine kinase (BTK)

2.1. Architecture of BTK

BTK belongs to the TEC family of nonreceptor protein-tyrosine kinases including BTK, BMX (bone marrow-expressed kinase), TEC (tyrosine kinases expressed in cellular carcinoma), ITK (inducible T cell kinase), and TXK (the X referred to an unknown kinase and TXK is also known as RLK, resting lymphocyte kinase) [17]. BTK contains a short N-terminal pleckstrin homology (PH) domain, a TEC homology (TH) domain, an SH3, SH2, and C-terminal protein kinase domain (Fig. 2 A), which is an architecture possessed by the other TEC family protein kinases. This architecture resembles that of the Src protein kinase family members except that they lack the PH and TH domains, but they contain a myristoylated N-terminal domain, which facilitates their binding to the inner plasma membrane (Fig. 2B) [18,19]. On the other hand, the PH domain of the TEC family binds to membrane-associated PIP_3, which accounts for their membrane-localization. Src possesses a C-terminal tail tyrosine phosphorylation site (pY530) that binds intramolecularly *in cis* with its SH2 domain to form an autoinhibited enzyme. BTK lacks this autoinhibitory tyrosine phosphorylation site suggesting that the mechanism for the interconversion of active and inactive BTK differs from that of Src, as described in Section 2.5.

BTK mediates the phosphorylation of protein-tyrosine residues in substrates such as PLCγ2. The PLCγ2 family possesses an intricate architecture consisting of an amino-terminal pleckstrin homology (PH) domain, four EF hands, a TIM-X domain, a second PH domain containing two SH2 and one SH3 domain followed by a TIM-Y domain, a C2 domain, and carboxyterminal H domain; the catalytic residues reside in the split TIM-X and TIM-Y segments (Fig. 2 C) [20]. The PLCγ2 phosphorylation sites (Y753, Y759) are found within the ^{751}SLYDVSRMYV^{760} sequence. These residues are found in the region between the second PLCγ2 SH2 domain and the SH3 domain. The following chemical equation gives the stoichiometry of the protein kinase reaction:

$$MgATP^{1-} + \text{protein–O:H} \rightarrow \text{protein–O:}PO_3^{2-} + MgADP + H^+$$

Note that the phosphorylium ion (PO_3^{2-}) is transferred from ATP to the protein substrate and not the phosphate (OPO_3^{2-}) group (I thank the late Fritz Lipmann (1899–1987) for pointing this out to me).

2.2. Primary structure of BTK

Hanks and Hunter investigated the primary structures of about 60 protein kinases from various families and divided them into 12 domains (I-VIA,VIB-XI) [21]. Protein kinase catalytic domains contain ≈ 250–300 amino acid residues. Domain I of BTK is designated as the glycine-rich loop (GRL) and it contains a GxGxΦG signature (^{409}GTGQFG^{414}), where Φ usually refers to a hydrophobic residue, and in the case of BTK this residue is phenylalanine. The G-rich loop links the β1- and β2-strands and covers the ATP-binding site. Owing to its participation in ATP binding and ADP release, the glycine-rich loop must be flexible. Domain II of BTK contains a conserved AxK (^{428}AIK^{430}) sequence in the β3-strand and domain III contains a conserved glutamate

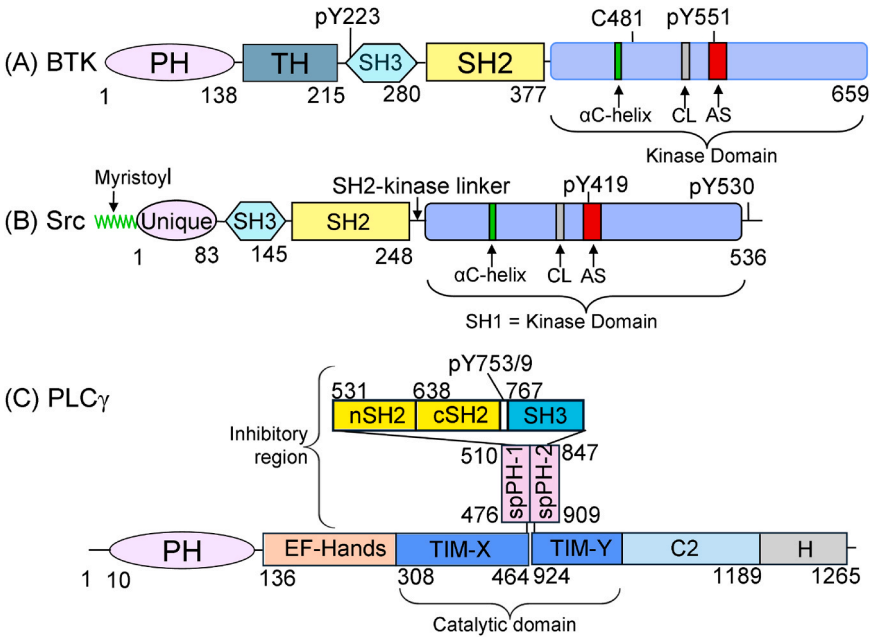

Fig. 2. (A) Architecture of Bruton protein-tyrosine kinase. (B) Architecture of Src. (C) Architecture of phospholipase Cγ. The relative size of each domain is indicated by the amino acid residue number. The BTK targeted covalent inhibitors bind to C481. AS, activation segment; CL, catalytic loop; PH, pleckstrin homology domain; pY, phosphotyrosine; TH, TEC homology domain; SH3, Src Homology domain 3; SH2, Src Homology domain 2. TIM, triose phosphate isomerase barrel-like; C2, Ca^{2+}-dependent membrane-binding loop.

(E455) in the αC-helix that forms a salt bridge with the conserved lysine while in the active protein kinase configuration. Domain VIB of BTK contains the catalytic loop (^{519}HRDLAARN^{526}) with a canonical HRD sequence. Domain VII contains a conserved ^{539}DFG^{541} sequence and domain VIII contains a ^{565}PPE^{568} sequence, which together represent the initial and final portion of the protein kinase activation segment. Note that an APE and not a PPE signature constitutes the end of the activation segment of most protein kinases. The αF–αI helices make up the final protein kinase domains. The X-ray crystal structure of PKA provided a helpful framework for understanding the role of the dozen domains on the protein kinase mechanism, as described next.

2.3. *The secondary and tertiary structure of BTK and the K/E/D/D motif*

The analysis of the X-ray crystal structure of the PKA catalytic subunit bound to a peptide protein kinase pseudosubstrate (antagonist) by Susan Taylor's group has clarified our views on the underlying biochemistry of the entire protein kinase enzyme family (PDB ID: 2CPK) [22,23]. All protein kinases including BTK have a small N-terminal lobe and large C-terminal lobe [24]. The small lobe contains five conserved β-strands (β1–5) and a regulatory αC-helix and the large lobe contains seven conserved helices (αD–αI and αEF) and four short β-strands (β6–β9). A cleft between the two lobes functions as the binding site for ATP, which is covered by the glycine-rich loop. Of the thousands of protein kinase domain structures that have been analyzed, all contain this fundamental protein kinase fold, which was first described for PKA [22,23].

Essentially all operational protein kinases contain a K/E/D/D (Lys/Glu/Asp/Asp) signature that plays crucial structural and mechanistic roles in the protein kinase reaction (Table 1) [25]. The lysine and glutamate residues occur within the amino-terminal lobe and the two aspartate residues occur within the carboxyterminal lobe. Although both lobes participate in ATP binding, the N-terminal lobe plays a key role in this process. K430 (the K of K/E/D/D) of the BTK β3-strand interacts with the α- and β-phosphates of ATP (not shown). The carboxylate moiety of E445 (the E of K/E/D/D) of the αC-helix forms a salt bridge with the ε-amino group of K430 and sustains its interactions with these

Table 1
Important residues in human BTK[a].

		Inferred function	Hanks no.[b]
N-lobe			
Glycine-rich loop: GxGxΦG	^{409}GTGQFG^{414}	Anchors ATP β-phosphate	I
β3-K (K of K/E/D/D)	K430	Forms salt bridges with ATP α- and β-phosphates	II
αC-E (E of K/E/D/D)	E475	Forms a salt bridge with β3-K	III
Hinge residues	^{475}EYMANG^{480}	Connects N- and C-lobes	V
C-lobe			
αE-AS loop and AS HΦ-interaction	F517-V546	Stabilizes the AS	VIb-VII
Catalytic loop HRD (first D of K/E/D/D)	D521	Catalytic base (abstracts proton)	VIb
Catalytic loop Asn (N)	N526	Chelates Mg^{2+}(2)	VIb
Activation segment	539–567	Positions the protein substrate	VII-VIII
AS DFG (second D of K/E/D/D)	D539	Chelates Mg^{2+}(1)	VII
AS phosphorylation site	Y551	Stabilizes the AS after phosphorylation	VIII
PPE, end of AS	565–567	Interacts with the αHI loop and stabilizes the AS	VIII
UniProt KB ID	Q06187		

[a] AS, activation segment
[b] From Ref. [21]

phosphates. The occurrence of an electrostatic bond between the β3-lysine and the αC-glutamate is necessary for the creation of the active protein kinase configuration, which corresponds to an "αC_{in}" structure (Fig. 3 A). However, when K430 and E475 fail to make contact, this represents an inactive enzyme with an "αC_{out}" structure (Fig. 3 C). The αC-in conformation is necessary, but not sufficient, for the manifestation of catalytic activity.

The C-terminal lobe binds to the protein substrate and contributes to the catalytic cycle. Two Mg^{2+} ions participate in the catalytic cycle of many protein kinases [19] and are probably necessary for the proper

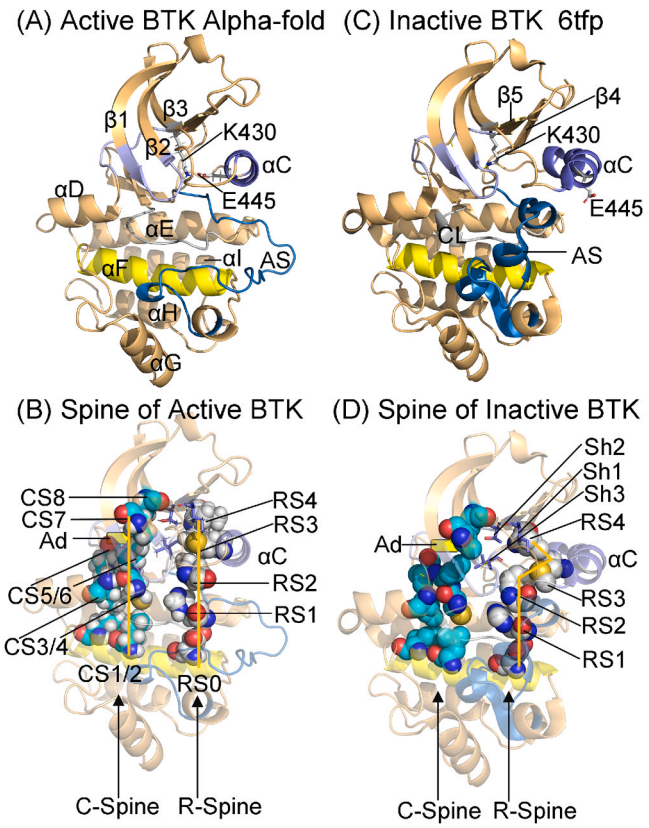

Fig. 3. (A) Overall structure of the active BTK protein-kinase domain. (B) Structure of the spines of active BTK. (C) Overall structure of the inactive BTK protein-kinase domain; PDB ID: 6tfp. (D The R-spine of an inactive BTK illustrating the displacement of RS3 as observed with the αC_{out} conformation. Ad, the adenine base; AS, activation segment; CL, catalytic loop. Figs. 3, 4, and 7 were prepared using PyMOL 2.5.4 Schrodinger, LLC.

functioning of BTK. By extension, DFG-D539 (the first D of K/E/D/D) binds to Mg^{2+}(1), which also binds to the β- and γ-phosphates of ATP. In the active enzyme, the DFG-D is directed inward (DFG-D_{in}) toward the active site. In an inactive conformation exhibited by many protein kinases, the DFG-D points away from the active site, the so-called DFG-D_{out} structure. BTK N526 of the catalytic loop binds Mg^{2+}(2), which in turn forms electrostatic bonds with the α- and γ-phosphates of ATP. The activation segment of catalytically competent BTK forms an open structure that mediates protein binding (Fig. 3 A). The activation segment of the inactive enzyme forms a closed, compact structure that disallows protein substrate binding (Fig. 3 C). Active and dormant BTK contain an αEF-helix near the end of the activation segment, a helix that occurs in most protein kinases. The exocyclic 6-amino group of ATP typically forms a hydrogen bond with the carbonyl backbone residue of the first hinge residue (BTK E475) that connects the N-terminal and C-terminal lobes of the protein kinase domain and the *N*1 nitrogen of the adenine base forms a second hydrogen bond with the N–H backbone of the third hinge residue (BTK M477). As noted later, most small-molecule steady-state ATP competitive inhibitors of protein kinases including BTK hydrogen bond with the backbone residues of the connecting hinge.

The protein kinase activation segment binds the protein substrate and promotes catalysis [26]. The BTK activation segment contains a phosphorylatable tyrosine. The segment is spatially located near the N-terminus of the αC-helix and the conserved catalytic loop HRD. These components interact hydrophobically. As with most protein kinases [27], phosphorylation of a residue within the activation segment (Y551 of BTK) promotes the conversion of an inactive enzyme to the active state [28]. The BTK activation segment and that of other protein kinases is further stabilized by hydrophobic interactions between an amino acid two residues amino-terminal to the HRD-H519 of the catalytic loop (F517) and seven residues C-terminal to the DFG-D539 (V546) within the activation segment.

The BTK catalytic loop near the actual site of phosphoryl transfer within the carboxyterminal lobe consists of ^{519}HRDLAARN^{526}. The BTK catalytic aspartate (D521), which is the first D of K/E/D/D, functions as a Lowry-Bronsted base that abstracts a proton from the tyrosyl –OH group (Fig. 4). The AAR sequence in the catalytic loop is found in many receptor protein-tyrosine kinases such as the platelet derived growth factor receptor and the epidermal growth factor receptor and RAA occurs in many nonreceptor protein-tyrosine kinases such as Src [21]. Accordingly, the occurrence of AAR in the BTK nonreceptor protein kinase catalytic loop is anomalous.

2.4. *Hydrophobic spines from active and inactive BTK*

Kornev et al. surveyed the three-dimensional structures of about two dozen active and inactive protein kinases and they identified crucial residues by a local spatial pattern alignment algorithm [29,30]. Their study led to a classification of eight hydrophobic residues as a catalytic or C-spine and four hydrophobic residues that constitute a regulatory or R-spine. Each spine consists of amino acids occurring in both the N-terminal and C-terminal lobes. The R-spine contains a residue from the activation segment and from the αC-helix, both of which are key elements in establishing active and dormant states. The adenine moiety of ATP forms part of the catalytic spine. The R-spine appropriately positions the protein substrate and the C-spine localizes ATP within the active site to facilitate catalytic activity. Furthermore, the appropriate assembly of both spines is necessary for the formation of an active protein kinase as described for protein-serine/threonine kinases, protein-tyrosine kinases, and MEK1/2 dual specificity protein kinases [13–15,31–39,41].

The classical protein kinase regulatory spine consists of the DFG-F of the activation segment, the HRD-H of the catalytic loop, a residue near the beginning of the β4-strand, and a residue near the carboxyterminal end of the αC-helix (four residues C-terminal to the conserved αC-glutamate) [29,30]. The backbone of the HRD-H is attached to the hydrophobic αF-helix by hydrogen bonding to a canonical aspartate residue. Going from the base to the apex of the R-spinal residues, Meharena et al. labeled them RS0, RS1, RS2, RS3, and RS4 (Figs. 3B and 3D) [40]. The R-spine of active BTK is rather linear while that of the inactive enzyme is nonlinear with the displacement of RS3.

The BTK C-spine consists of residues from both the amino-terminal and carboxyterminal lobes and it is completed by the adenine base of ATP (Fig. 3B) [30]. The two residues of the N-terminal lobe of protein kinase domains that interact with the ATP adenine include a canonical

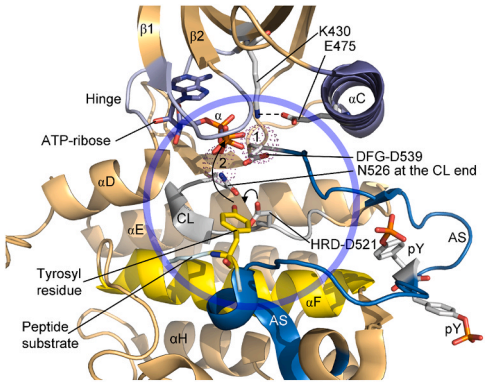

Fig. 4. Mechanism of the BTK catalyzed reaction. The chemistry occurs within the blue circle. AS, activation segment; CL, catalytic loop; pY, phosphotyrosine. The spheres labeled 1 and 2 represent Mg^{2+}(1) and Mg^{2+}(2), respectively. Prepared from PDB ID: 2pvf.

valine at the beginning of the β2-strand (CS7) and a conserved alanine from the AxK signature of the β3-strand (CS8). Moreover, a hydrophobic residue from the β7-strand (CS6) interacts with the adenine moiety. The CS6 residue is buttressed by two hydrophobic residues (CS4 and CS5) that interact hydrophobically with the CS3 residue near the origin of the αD-helix. These three residues (CS4/5/6) occur after the asparagine terminus of the catalytic loop (HRDxxxxN). Lastly, CS3 and CS4 interact with the CS1 and CS2 residues of the αF-helix to complete the C-spine (Figs. 3B and 3D) [41]. Of importance, the internal hydrophobic αF-helix anchors both the catalytic and regulatory spines. Moreover, both spines play a critical role in placing the enzymatic catalytic residues in their active conformation. When assessing the location of the spinal residues, the chief divergence between active and dormant BTK domains involves RS3.

Based upon site-directed mutagenesis studies, Meharena et al. identified three residues in protein kinase A that support the R-spine, which they named Sh1, Sh2, and Sh3, where Sh refers to shell [40]. (See Fig. 3D for the location of the BTK shell residues). The Sh2 residue is the gatekeeper residue. The term gatekeeper specifies the role that this amino acid plays in regulating access to a back cleft [42], which is also called the back pocket or hydrophobic pocket II (HPII). The amino acids that constitute the spines were established by their location in active and dormant kinases based upon their X-ray crystal structures [29,30]. This contrasts with the determination of the HRD, DFG, or APE signatures, which was based upon their primary structure [21]. Table 2 lists the spine and shell residues of BTK. Of importance in examining drug interactions and specificity, small molecule protein kinase therapeutic blockers generally interact with many residues that make up the spine and shell residues including RS2/3, Sh2/3, CS7/8, and the KLIFS-3 residue [41].

Modi and Dunbrack described eight different protein kinase conformations and classified them based upon the structure of the phenylalanine rotamer (plus, minus, trans) and on the Ramachandran regions (A, alpha; B, beta; L, left) of the xDF motif [43]. Their classification system divides the DFG-D_{in} configuration into six clusters including BLAminus, which represents an active structure and five dormant or inactive conformations. These investigators created a useful searchable and noncommercial web site (https://dunbrack.fccc.edu/kincore/) that allows one to determine whether a given protein kinase structure corresponds to an active or dormant enzyme. We used the kincore web site to determine whether the structures of our drug-enzyme complexes correspond to active (BLAminus) or inactive (otherwise) conformations.

Table 2
Spine and shell residues of murine PKA and human BTK.

	Symbol	PKA[a]	BTK
Regulatory spine			
β4-strand (N-lobe)	RS4	L106	L460
C-helix (N-lobe)	RS3	L95	M449
Activation loop F of DFG (C-lobe)	RS2	F185	F540
Catalytic loop Y/H (C-lobe)	RS1	Y164	H519
F-helix (C-lobe)	RS0	D220	D579
Shell			
Two residues upstream from the gatekeeper	Sh3	M118	I472
Gatekeeper, end of β5-strand	Sh2	M120	T474
αC-β4 loop	Sh1	V104	V458
Catalytic spine			
β3-AxK motif (N-lobe)	CS8	A70	A428
β2-strand (N-lobe)	CS7	V57	V416
β7-strand (C-lobe)	CS6	L173	L528
β7-strand (C-lobe)	CS5	I174	V529
β7-strand (C-lobe)	CS4	L172	C527
αD-helix (C-lobe)	CS3	M128	L482
αF-helix (C-lobe)	CS2	L227	L586
αF-helix (C-lobe)	CS1	M231	I590

[a] From Refs. [29,30,40].

2.5. Interconversion of inactive and active BTK

Wang et al. performed structural and biochemical studies on BTK that revealed the molecular mechanism of its autoinhibition and reactivation [44]. Although the general modular components of BTK and Src are similar (Fig. 2 A/B), the former contains an N-terminal PH-TH domain, but it lacks an inhibitory carboxyterminal phosphorylation site. Despite these dissimilarities, autoinhibited BTK possesses a compact structure that resembles that of the Src family kinases. The PH-TH module binds PIP_3 at a canonical binding site and IP_6 (inositol 1,2,3,4,5,6-hexakisphosphate) binds at a peripheral site. The PH-TH module functions in combination with the SH2 and SH3 domains to strengthen the inactive conformation (Fig. 5). The PH-TH domain binds in a channel between αC-helix and the kinase linker. This interface stabilizes the inactive conformation and blocks the translation of the αC-helix that is required to form the active αC_{in} structure. The SH3 domain interfaces with a polyproline type-II helix found within the SH2-kinase linker segment, which in turn interfaces with and stabilizes the small lobe of the protein kinase domain. The SH2 domain interacts with both the large lobe and carboxyterminal tail while the PH-TH domain interacts with and immobilizes the small lobe.

Following the activation of PI3K by the B cell receptor and the resulting formation of PIP_3, Wang et al. reported that the PIP_3-binding site in the PH-TH module is drawn to the plasma membrane by a procedure that reverses the compressed inactive conformation [44]. The interaction of two enzyme molecules leads to the *trans*-phosphorylation of Y551 within the activation segment of one or both enzymes and generates the active state. The phosphorylation of Y223 within the SH3 domain also occurs. However, this alteration fails to modify the enzymatic activity of BTK, but it may modify the selectivity toward its binding partners. Activated BTK participates in signal transduction as outlined in Fig. 1. Wang et al. reported that the hydrophilic IP_6 interfaces with a BTK peripheral binding site and promotes dimer formation in a membrane-independent process producing the ATP-dependent *trans*-phosphorylation of the activation segment and enzyme activation [44]. The pathway for the conversion of the active phosphorylated BTK to the inactive conformation likely involves dephosphorylation of pY551 within the activation segment and detachment of the enzyme from membrane-associated PIP_3 followed by dephosphorylation of PIP_3.

3. Disorders treated with Bruton tyrosine kinase (BTK) blockers

3.1. Mantle cell lymphoma (MCL)

Patients with MCL, which makes up about 6% of non-Hodgkin lymphoma patients, most commonly present at a median age of about 65 years with palpable lymphadenopathy [45,46]. The male/female ratio is 4/1. Almost 70% of patients are at stage IV at the time of diagnosis with bone marrow, peripheral blood, spleen, and gastrointestinal pathology. The median overall survival in patients with newly diagnosed MCL is three to five years. The genetic hallmark of these B cell lymphomas is a t(11;14) (q13;q32) chromosomal translocation involving the Ig heavy chain gene on chromosome 14 and the *CCND1* gene on chromosome 11, which causes the overexpression of cyclin D1. Cyclin D1, in turn, activates CDK4 and CDK6 thereby promoting G1-S cell cycle progression [32]. The structural component of lymphatic tissue is the lymphatic nodule, which consists of a germinal center and a mantle or outer ring of small lymphocytes that is the initial location of the cells of this lymphoma. Therapies for mantle cell lymphoma include (i) the rituximab-CHOP regimen of cyclophosphamide, hydroxydaunorubicin (doxorubicin, adriamycin), oncovin (vincristine), and prednisone combined with rituximab, (ii) Hyper-CVAD cyclophosphamide, vincristine, adriamycin (doxorubicin), and dexamethasone alternating with high-dose cytarabine and methotrexate) without or with rituximab (R-Hyper-CVAD), (iii) bortezomib, (iv) lenalidomide, (v) or

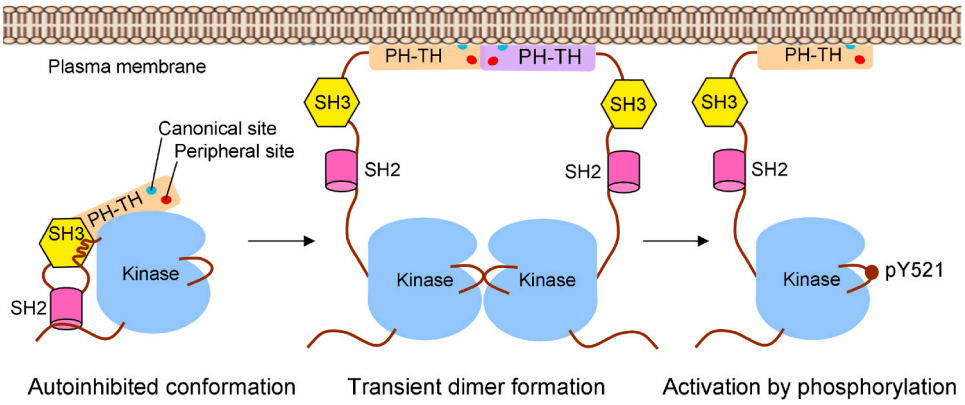

Fig. 5. Conversion of inactive to active BTK following recruitment by PIP_3 to the plasma membrane. PH-TH, pleckstrin homology-TEC homology domain. Adapted from Ref. [44].

temsirolimus [47]. See Table 3 for the mechanism of action of these agents. Three BTK inhibitors are FDA-approved for the treatment of mantle cell lymphoma including acalabrutinib, pirtobrutinib, and zanubrutinib (Table 4). Ibrutinib was approved for the treatment of MCL in 2013, but this was withdrawn by the manufacturer in 2023 because it failed to meet the overall survival endpoint. CAR T-cell therapies (lisocabtagene maraleucel or brexucabtagene autoleucel) are also used in the management of relapsed/refractory mantle cell lymphoma [48]. See Refs. [45–48] for a summary of the clinical studies that led to the approval of these medicines.

3.2. *Chronic lymphocytic leukemia (CLL) and small lymphocytic lymphoma (SLL)*

The bone marrow of patients with CLL produces nonfunctional lymphocytes [49,50]. CLL is the most widespread leukemia in the Western hemisphere and accounts for about 40% of all adult leukemias. The age-adjusted incidence rate of this clonal B cell disorder is 4.5 per 100,000 residents of the United States, which amounts to about 15,000 new cases per year. The median age at the time of diagnosis is about 70 years. Its diagnosis is often incidental and is based upon routine blood counts. Fatigue, fever, and infections may be the presenting features in those patients with symptoms. Physical examination reveals axillary, cervical, and inguinal lymphadenopathy in about 80% of patients and splenomegaly and hepatomegaly in about 50% of patients. About 5% of CLL patients progress into an aggressive large cell lymphoma (LCL) by a transformation that is called Richter syndrome. Laboratory studies indicate that CLL and LCL cells share identical clonal origins. SLL is basically the same as CLL, but SLL involves the accumulation of nonfunctional cells in the lymph nodes as opposed to the bone marrow

CLL patients exhibit elevated lymphocyte counts with more than 5000 nonproliferating clonal B cells/μL lasting more than three months [49,50]. Monoclonal B cell lymphocytosis is characterized by fewer than 5000 cells/μL and is regarded as a precursor to CLL. These immune-incompetent cells exhibit (i) little cytoplasm, (ii) dense chromatin, and (iii) they lack nucleoli. These cells express CD5 and CD19 B cell markers, a finding commonly observed in CLL and MCL. MCL is distinguished from CLL by the expression of CD23, CD20, CD200 and LEF-1 in the latter. Recombination of variable (V), diversity (D), and joining (J) genes occurs in the pre-germinal phase of B cell development. Somatic mutations are introduced in the VDJ rearrangement in normal B cells. Approximately 50% of CLL cases have somatic mutations in the IgV gene (*IGHV-M*) and thus arise from post-germinal B cells while a subset of CLL has unmutated IgV (*IGHV-UM*) that arises from naïve B cells. *IGHV-M* CLLs respond poorly to surface membrane immunoglobulin stimulation, but CLL patients with this mutation have a favorable outcome. Patients with *IGHV-UM* do less well and require earlier treatment.

The management of CLL is evolving as several targeted agents are currently available [50]. Patients with low risk CLL can be followed without specific therapy (watchful waiting) with a median survival of 10 – 15 years [51]. Indications for treatment include symptomatic lymphadenopathy, thrombocytopenia, anemia, and progressive fatigue. These patients have stage II disease or stage III/IV disease. There are a variety of initial CLL treatments. Options include a BTK inhibitor (acalabrutinib, ibrutinib, zanubrutinib) as a single agent or venetoclax (a Bcl-2 inhibitor resulting in apoptosis) in combination with an anti-CD20 antibody (obinutuzumab, ofatumumab, rituximab). The choice among these agents is based on patient or physician preference or toxicity. The BTK blockers are orally bioavailable and require continuous dosing. They are well tolerated but can be associated with atrial fibrillation, hypertension, ventricular arrhythmias, and bleeding. The incidence of cardiovascular complications is greater with ibrutinib and lesser with acalabrutinib or zanubrutinib. Venetoclax is usually given for a self-limited course of therapy and is associated with tumor lysis syndrome and neutropenia. Traditional combination FDA-approved chemotherapy is used only in selected cases including chlorambucil (approved in 1957), cyclophosphamide (1959), fludarabine (1991), alemtuzumab (2007), bendamustine (2008), ofatumumab (2009), rituximab in combination with fludarabine and cyclophosphamide (2010), obinutuzumab in combination with chlorambucil (2013) [51], and idelalisib (2014). The mechanism of action of these agents is provided in Table 3. See Refs. [50,52] for a summary of clinical trials that led to the approval of various CLL therapies.

Patients taking a BTK blocker who develop resistance and relapse should undergo testing to identify recurrent BTK pathogenic variants (e.g., *C481S*) that may respond to pirtobrutinib [50,53]. An alternative resistance treatment includes the combination of venetoclax with an anti-CD20 antibody. For people who relapse on venetoclax-based therapy, BTK blockers are often prescribed. Chimeric antigen receptor T-cell (CAR-T cell) therapy represents another option for the management of refractory CLL patients and can produce long-lasting remissions. Finally, allogeneic transplantation can offer a potentially curative treatment of patients with CLL, but it should be used only in patients whose disease cannot be controlled by the available therapies owing to the high morbidity and mortality associated with this approach. Patients with stage 0 or stage I disease have a median survival of greater than ten years. Patients with stage III or stage IV disease had a median survival of less than two years in the past, but with current treatment modalities, five-year survival is more than 70% and the long-term outlook is substantially improved.

Table 3
Synopsis of drugs and biologics used in the treatment of various hematologic and immune disorders [a].

Drug	Diseases	Targets	Mechanism
Small molecule agents, MW (Da)			
Acalabrutinib, 466	CLL, SLL, MCL	BTK	Orally effective irreversible BTK inhibitor
Asciminib, 450	Ph^+ CML	BCR-Abl	Orally bioavailable BCR-Abl blocker
Bortezomib, 384	MCL, MM	Proteosome	IV injectable proteosome inhibitor
Bosutinib, 530	Ph^+ CML	BCR-Abl	Orally bioavailable BCR-Abl blocker
Buparlisib, 410	MCL, Breast cancer	PI3 kinase	Orally effective pan-PI3 kinase inhibitor
Carfilzomib, 720	MM	Proteosome	IV injectable proteosome inhibitor
Crizotinib, 450	ALK^+ (i) anaplastic large cell lymphoma, (ii) inflammatory myofibroblastic tumors	ALK, ROS1	Orally effective ALK and ROS1 blocker
Dasatinib, 488	ALL, CML	BCR-Abl, BTK, Src, Lck, Yes, Fyn, Kit, EphA2, PDGFRβ	Orally bioavailable multi-protein kinase inhibitor
Dexamethasone, 392	Inflammatory and neoplastic diseases	Immune system	Orally effective glucocorticoid immunosuppressant
Fedratinib, 525	Primary or secondary myelofibrosis	JAK2	Orally bioavailable JAK inhibitor
Fostamatinib, 580	Chronic immune thrombocytopenia	Syk	Orally effective Syk blocker
Gilteritinib, 553	*FLT3*-mutation positive AML	Flt3	Orally effective Flt3 inhibitor
Ibrutinib, 441	CLL, SLL, WM, GVHD	BTK	Orally bioavailable irreversible BTK inhibitor
Idelalisib, 415	CLL, FL, SLL	PI3 kinase-δ inhibitor	Orally effective PI3 kinase-δ inhibitor
Imatinib, 494	Ph^+ CML ALL, or MDS (with *PDGFR* gene rearrangements); aggressive systemic mastocytosis, chronic eosinophilic leukemia, hypereosinophilic syndrome, *KIT* mutation-positive GIST, dermatofibrosarcoma protuberans, and as a second-line treatment for aggressive systemic mastocytosis without the KIT^{D816V} mutation	BCR-Abl	Orally effective BCR-Abl and multi-kinase inhibitor
Lenalidomide, 259	MM, MDS, MCL, FL, MZ	E3 ubiquitin ligase	Orally bioavailable immunomodulatory drug that promotes the binding of cereblon E3 ubiquitin ligase complex to IKZF1/3 transcription factors leading to their degradation
Midostaurin, 571	*FLT3* mutation positive AML, mastocytosis, mast cell leukemia	Flt3	Orally effective Flt3 blocker
Momelotinib, 414	Primary or secondary myelofibrosis patients with anemia	JAK1/2	Orally bioavailable JAK inhibitor
Nilotinib, 530	First or second-line treatment of Ph^+ CML	BCR-Abl	Orally effective BCR-Abl blocker
Pacritinib, 473	Myelofibrosis with a low platelet count	JAK2	Orally bioavailable JAK2 inhibitor
Pirtobrutinib, 479	MCL, CLL, SLL	BTK	Orally bioavailable BTK blocker
Ponatinib, 533	Ph^+ ALL, CML, $T315I^+$ CML	BCR-Abl	Orally effective BCR-Abl inhibitor
Pomalidomide, 273	MM, AIDS-related Kaposi sarcoma	E3 ubiquitin ligase	Orally bioavailable immunomodulatory drug that promotes the binding of cereblon E3 ubiquitin ligase complex to IKZF1/3 transcription factors leading to their degradation
Prednisone, 358	Inflammatory and neoplastic diseases	Immune system	Orally bioavailable glucocorticoid immunosuppressant; the P of the CHOP, CVP, and COP regimens
Quizartinib, 561	*FLT3* internal tandem duplication positive AML	Flt3	Orally bioavailable Flt3 blocker
Remibrutinib, 508	Chronic spontaneous urticaria	BTK	Orally effective BTK blocker
Rilzabrutinib, 666	Chronic immune thrombocytopenia	BTK	Orally effective BTK blocker
Ruxolitinib, 306	Myelofibrosis, polycythemia vera, graft vs. host disease	JAK family	Orally bioavailable JAK inhibitor
Selinexor, 443	MM, DLBCL	Nuclear export	Orally effective nuclear export inhibitor that prevents tumor suppressor proteins from exiting the nucleus
Temsirolimus, 1030	MCL (off-label)	MKBP1/2 mTOR	IV injectable MKBP12/mTOR inhibitor
Venetoclax, 868	CLL, SLL, AML	Apoptosis and Bcl-2	Orally bioavailable small molecule inhibitor of Bcl-2 leading to apoptosis, a BH3-mimetic
Zanubrutinib, 472	MCL, CLL, SLL, WM, FL, MZL	BTK	Orally bioavailable irreversible BTK blocker
Cytotoxic agents, MW (Da)			
Bendamustine, 358	CLL, indolent B cell NHL	DNA	IV injectable DNA alkylating agent related to nitrogen mustards
Chlorambucil, 304	CLL, NHL, HD	DNA	Orally effective nitrogen mustard alkylating agent.
Cyclophosphamide, 251	HD, NHL, Burkitt lymphoma, CLL, CML, AML, ALL, Breast, Ovary	DNA	Similar to bendamustine except it can be given orally; part of the CHOP, R-FC, FCM, CVP, and COP regimens
Cytarabine, 243	AML, ALL	DNA & RNA polymerases	IV injectable inhibitor of DNA and RNA polymerases and DNA replication
Etoposide, 589	HD, NHL, AML, ALL, DLBCL	DNA topoisomerase II	IV injectable DNA topoisomerase II inhibitor that causes DNA strand breakage; part of the MINE regimen
Gemcitabine, 263	Cutaneous T-cell lymphoma	Ribonucleotide reductase	IV injectable nucleoside analog that inhibits ribonucleotide reductase and then DNA synthesis
Doxorubicin (hydroxydaunorubicin, adriamycin), 544	HD, HL, NHL, ALL, AML, CLL	DNA topoisomerase II	IV injectable drug that intercalates with DNA and inhibits the progression of topoisomerase II thereby inhibiting DNA replication; part of the CHOP regimen
Fludarabine, 285	CLL, NHL	Ribonucleotide reductase, DNA polymerase α, DNA primase	IV injectable purine analog that inhibits ribonucleotide reductase and DNA polymerase-α thereby inhibiting DNA synthesis; part of the R-FC and FCN regimens
Idarubicin, 497	AML, ALL	DNA topoisomerase II	IV injectable drug that intercalates with DNA and inhibits the progression of topoisomerase II thereby inhibiting DNA replication; related to doxorubicin

(*continued on next page*)

Table 3 (*continued*)

Drug	Diseases	Targets	Mechanism
Ifosfamide, 261	NHL, DLBCL	DNA	IV injectable DNA alkylating agent; part of the MINE regimen
Methotrexate, 454	ALL, NHL, other cancers, many inflammatory diseases	Dihydrofolate reductase	Orally effective agent that inhibits dihydrofolate reductase thereby decreasing the synthesis of tetrahydrofolate, which is required for the synthesis of thymidine as well as the purine and pyrimidine bases
Novantrone (mitoxantrone), 444	Used off-label for FL; FDA-approved for MS and acute non-lymphocytic leukemia	DNA	Intercalates into DNA, inhibits topoisomerase II, and induces DNA strand breaks, which triggers apoptosis; part of the FCM and MINE regimens
Oncovin (vincristine), 825	ALL, AML, CLL, HD, neuroblastoma, SCLC	Microtubules	IV injectable drug that binds to microtubules blocking metaphase; part of the CHOP, CVP, and COP regimens
Monoclonal antibodies and recombinant fusion proteins (given parenterally)			
Abatacept	GVHD	CD80, CD86	Abatacept is a recombinant fusion protein composed of the extracellular domain of cytotoxic T-lymphocyte-associated antigen 4 (CTLA-4) and the Fc portion of immunoglobulin G1 (IgG1)
Alemtuzumab	CLL, MS	CD52	A humanized monoclonal IgG1 antibody directed against CD52, which occurs on mature T and B lymphocytes
Axatilimab-csfr	Third-line treatment of GVHD	CSF1 receptor	A humanized IgG4 monoclonal antibody that acts as a colony-stimulating factor-1 receptor (CSF-1R) inhibitor on monocytes and macrophages, blocking their activation and survival. This decreases tissue inflammation and fibrosis in chronic GVHD.
Obinutuzumab	CLL, FL	CD20	A humanized monoclonal antibody directed against CD20, which is found primarily on the surface of B cells; part of the O-CHOP and O-B (bendamustine) regimens
Ofatumumab	CLL, MS, WM (off-label)	CD20	A fully human monoclonal antibody directed against CD20.
Rituximab	CLL, NHL, RA, Wegener granulomatosis	CD20	A chimeric monoclonal antibody directed against CD20; part of the R-FC regimen
Tafasitamab	Relapsed/refractory FL	CD19	The humanized monoclonal antibody binds to CD19, leading to antibody-dependent cellular cytotoxicity (ADCC) and antibody-dependent cellular phagocytosis (ADCP) by natural killer (NK) cells and macrophages. Prescribed with rituximab and lenalidomide.
CAR T-cell therapies			
Axicabtagene ciloleucel	Second-line treatment of DLBCL and FL	CD19	An autologous CD19-directed CAR T-cell therapy that reprograms T cells to express a chimeric antigen receptor (CAR). It uses a CD28 costimulatory domain to enhance expansion, binding to CD19-positive cells to trigger T-cell activation, cytokine release, and tumor cell apoptosis
Lisocabtagene maraleucel	Second-line and later treatment of DLBCL, FL, and relapsed/refractory MZL	CD19	Same as above
Tisagenlecleucel	Third-line treatment of FL, ALL, DLBCL	CD19	Same as above

[a] ALL, acute lymphocytic leukemia; AML, acute myelogenous leukemia; DLBCL, diffuse large B cell lymphoma; CHOP; cyclophosphamide, hydroxydaunorubicin, oncovin (vincristine), prednisone; CML, chronic myelogenous leukemia; CVP, cyclophosphamide, vincristine, prednisone; CLL, chronic lymphocytic leukemia; COP, cyclophosphamide, oncovin, prednisone; FCM, fludarabine, cyclophosphamide, mitoxantrone; FL, follicular B cell non-Hodgkin lymphoma; GIST, gastrointestinal stromal tumor; GVHD, graft vs host disease; HD, Hodgkin disease; HL, hairy cell leukemia; IV, intravenous; MCL, mantle cell lymphoma; MDS, myelodysplastic syndrome: MINE, mensa (sodium 2-mercaptoethane sulfonate), ifosfamide, novantrone (mitoxantrone), etoposide; MM, multiple myeloma; MS, multiple sclerosis; MW, molecular weight; MZL, marginal zone lymphoma; NHL, non-Hodgkin lymphoma; Ph^+, Philadelphia-chromosome positive; PI, phosphatidyl inositol; R-FC, rituximab, fludarabine, cyclophosphamide; RA, rheumatoid arthritis; SCLC, small cell lung cancer; SLL, small lymphocytic lymphoma; WM, Waldenström macroglobulinemia

Table 4
FDA-approved small molecule Bruton tyrosine kinase inhibitors and their therapeutic indications[a].

Drug	Code	Company	Trade name	Year approved	Therapeutic indications (date of FDA label)[b]
Ibrutinib	PCI-32765	Johnson & Johnson	Imbruvica	2013	CLL, SLL, Waldenström macroglobulinemia, second line treatment of graft vs. host disease (October 2025)
Acalabrutinib	ACP-196	Acerta Pharma	Calquence	2017	CLL, SLL, first-line treatment of MCL in combination with bendamustine and rituximab in patients who are ineligible for autologous hematopoietic stem cell transplantation, second-line treatment of MCL (January 2025)
Zanubrutinib	BGB3111	BeiGene	Brukinsa	2019	CLL, SLL, Waldenström macroglobulinemia, second-line treatment of MCL, relapsed or refractory FL - in combination with obinutuzumab - after two or more lines of systemic therapy, relapsed or refractory MZL in patients who have received at least one anti-CD20–based regimen (June 2025)
Pirtobrutinib	LOXO-305	Lilly	Jaypirca	2023	Second and third-line treatment of CLL, SLL, MCL (December 2025)
Remibrutinib	LUO064	Novartis	Rapsido	2025	Chronic spontaneous urticaria (September 2025)
Rilzabrutinib	PRN1088	Genzyme	Wayritz	2025	Chronic immune thrombocytopenia (August 2025)

[a] Data from Refs. [10–16] and www.brimr.org/PKI/PKIs.htm.
[b] CLL, chronic lymphocytic leukemia; FL, follicular lymphoma; MCL, mantle cell lymphoma; MZL, marginal zone lymphoma; SLL, small lymphocytic lymphoma.

3.3. Waldenström macroglobulinemia (WM)

WM is a B cell neoplasm characterized by the accumulation of clonal immunoglobulin M secreting lymphoplasmacytic cells [54]. The age-adjusted incidence rate is about 0.38 per 100,000 inhabitants in the United States, which amounts to about 1250 cases per year. The median age at the time of diagnosis is about ≈ 70 years of age and the male/female ratio is about 3/2. This disease is heterogeneous and can present with fever and chills, fatigue, recurrent sinus and bronchial infections, headaches, gastrointestinal cramping, and diarrhea. Physical examination may reveal hepatosplenomegaly and lymphadenopathy. Elevated IgM levels (>7 g/dL) are more than 25 times the normal value. These high levels lead to increased serum viscosity, which may manifest itself as blurry vision, headaches, episodes of mental confusion, and nose bleeds. The occurrence of IgM monoclonal protein associated with more than 10% of clonal lymphoplasmacytic cells in the bone marrow will corroborate the diagnosis.

An L265P *MYD88* (myeloid differentiation primary response gene 88) mutation occurs in more than 90% of patients [55]. This gene product is an adapter protein that facilitates innate immune responses and Toll-like receptor signaling. This gain-of-function mutation contributes to the activation of NF-κB by means of BTK (Fig. 1) and the IL-1 receptor-associated kinases (IRAK1 and IRAK4). Owing to the *MYD88* mutation, BTK is constitutively activated in WM cells. Mutations in the *CXCR4* chemokine receptor occur in about one-third of these patients. These mutations resemble those in patients with the WHIM syndrome (warts, hypogammaglobulinemia, infections, and myelokathexis, where the latter expression signifies the retention – kethexis – of neutrophils in the bone marrow). CXCR4 receptor activation mediates lymphocyte chemotaxis.

An assortment of therapies is used in the management of Waldenström macroglobulinemia [54,56–58]. These include rituximab (an anti-CD20 monoclonal antibody), as a first-line treatment alone or in combination with ibrutinib as a chemotherapy-free regimen. The combination of rituximab with other agents (bendamustine, bortezomib, dexamethasone and cyclophosphamide) is generally more effective than rituximab monotherapy. The BTK inhibitor zanubrutinib is an approved monotherapy for the treatment of WM. Ibrutinib is FDA-approved for the management of Waldenström macroglobulinemia (WM) both as a single agent (monotherapy) and in combination with rituximab. The rituximab-CHOP (cyclophosphamide, hydroxydaunorubicin, oncovin, prednisone) protocol is used off-label for the treatment of WM, but it is associated with peripheral neuropathy and myelosuppression.

The choice of therapies for Waldenström macroglobulinemia depends upon specific patient factors, genetic profiles, and treatment goals while none of the therapies is universally superior [57]. The combination of rituximab and chemotherapy (bendamustine or dexamethasone with cyclophosphamide) is a fixed-duration treatment (four–six months) that allows for treatment-free periods. BTK blockers are continuous therapies taken indefinitely until there is disease progression or limiting toxicity. They have reduced efficacy in patients with wild-type MYD88 or in patients with *CXCR4* mutations. They carry the risk of atrial fibrillation, hypertension, and bleeding. On the other hand, BTK inhibitors are considered among the most active single agents with rapid and long-lasting responses. Chemoimmunotherapy may be preferred for patients with bulky lymphadenopathy, but it can cause myelosuppression. See Refs. [54–58] for a summary of the clinical studies leading to the approval of these medicines.

3.4. Follicular lymphoma (FL)

FL is the most common form of indolent non-Hodgkin lymphoma in the United States [59]. The estimated annual incidence in the United States is about 15,000 – 20,000 and accounts for about 20% of all lymphomas. It is less common in Europe and is rare in Asian populations. Follicular lymphoma patients present in middle age (median age at diagnosis, 60 years); it affects males and females equally and is characterized by prolonged overall survival reaching or exceeding 20 years. Although patients usually respond well to treatment, most will experience relapses. FL arises from cells at the center of the lymph node lymphoid follicle and is characterized by a nodular or follicular growth pattern similar to that of the germinal centers.

The excisional biopsy of a lymph node or an affected tissue is the gold standard for making a diagnosis of follicular lymphoma [60]. FL cells express CD10, CD19, CD20, CD22, CD79a, Bcl-2, and Bcl-6. The t(14;18)(q32;q21) translocation produces the rearrangement of the *BCL* gene with the promoter of the Ig heavy (IGH) chain gene. The patient's workup includes a medical history including the assessment of B symptoms (fever, night sweats, and weight loss) and basic laboratory tests including lactate dehydrogenase and β2-microglobulin. PET-CT is the standard imaging procedure for initial disease staging and response evaluation. A bone marrow biopsy is a necessary component of the diagnostic workup.

The initial management of follicular lymphomas depends upon whether the disease is localized or advanced at the time of diagnosis [60–62]. Those patients with localized disease and a low tumor burden are treated with watchful waiting or radiation therapy alone or in combination with rituximab. Patients with a high tumor burden require active management. Possibilities include immunochemotherapy (rituximab-CHOP, rituximab-CVP, or rituximab-bendamustine). For those patients who achieve a complete or partial response, maintenance with an anti-CD20 antibody (every two months for a maximum of two years) is a recommended option. For patients with relapses following immunochemotherapy, treatment with a different immunochemotherapy from that used in the first line setting is a viable alternative. Other possibilities include rituximab with lenalidomide. Second or subsequent relapses can be treated with previously not used immunochemotherapy, rituximab-lenalidomide with or without tafasitamab (Table 3), bispecific CD3 x CD20 antibodies (epcoritamab or mosunetuzumab), and CAR T-cell therapies (lisocabtagene maraleucel, axicabtagene ciloleucel, tisagenlecleucel). The only BTK inhibitor approved for the treatment of relaxed/refractory follicular lymphoma is zanubrutinib in combination with obinutuzumab (a humanized anti-CD20 antibody) [63]. See Refs. [59–62] for a summary of the clinical findings that led to the approval of these therapies.

3.5. Marginal zone lymphomas (MZLs)

MZLs are the third most common indolent non-Hodgkin lymphoma making up somewhat less than 10% of NHL cases [64]. These patients usually present at a median age of 60 years with a slight bias toward females. Extranodal MZL of mucosa-associated lymphoid tissue (MALT), nodal MZL, and splenic B cell MZL constitute the three major subtypes of this disorder. The relative incidence of these non-Hodgkin lymphomas is 7%, 2%, and less than 1%, respectively.

The most common site of MALT involvement is the stomach, but other sites can be involved including the lung, skin, salivary gland, GI tract, and thyroid [64]. Patients often present with signs and symptoms of peptic ulcer disease including epigastric pain and dyspepsia. Anemia, weight loss, and GI bleeding are observed in people with more advanced disease. *H. pylori* occurs in the gastric mucosa of many patients with MALT lymphoma and its elimination results in the regression of this lymphoma in more than half of patients. The MALT lymphomas express monotypic Ig light chain, B cell antigens, and Bcl-2. These lymphomas possess t(11;18)(q21,q21), t(14;18)(q32;q21), t(1;14)(p22;q32), t(3;14)(p14.1;q32), and t(2,7)(p11;q21) chromosomal translocations. These translocations alter signaling associated with cell proliferation or with the blockade of apoptosis. Activation of NF-κB is common. Surgery and radiation therapy are prime therapeutic approaches for localized MALT that fails to respond to antibiotic therapy and in patients with *H. pylori*–negative disease. The BTK blocker zanubrutinib is FDA approved for this malady [63].

Patients with nodal MZL generally present with peripheral or para-aortic lymphadenopathy [64]. Not surprisingly, these lymphomas have a propensity to involve the marginal zones of lymph nodes. In most cases the neoplasm expands into the perifollicular compartments with the sparing of germinal centers. Nodal MZLs are mature B cell neoplasms that express monocytic Ig, pan–B cell antigens, and Bcl-2. They do not express CD10, CD21, CD23, Bcl-6, cyclin D1, or T-cell antigens including CD5. Moreover, they fail to express the translocations observed in MALT lymphomas.

Patients with splenic MZL usually present with splenomegaly, cytopenias, and circulating malignant lymphocytes. Bone marrow involvement is common, but peripheral lymphadenopathy and B symptoms are rare. The clinical course is indolent with a five-year overall survival rate of about 70%. Splenectomy is indicated for people with symptomatic splenomegaly or cytopenias secondary to hypersplenism. The best treatment for splenic MZL includes rituximab (monotherapy or with chemotherapy), which provides high response rates and long-term survival, while chemoimmunotherapy (e.g., rituximab-CHOP, rituximab-bendamustine) is used for more advanced cases. The BTK blocker zanubrutinib is FDA-approved for the second-line treatment of marginal zone lymphoma [63]. See Refs. [65,66] for a summary of the clinical trials that led to the approval of these therapies.

3.6. *Graft vs. host disease (GVHD)*

GVHD is a serious, potentially fatal complication where donor immune cells (the graft) attack the recipient (the host) after the transplantation of an allogeneic (genetically dissimilar) stem cell [67]. GVHD commonly affects the skin, liver, and intestines. Patients typically suffer from skin rash, itching, abdominal pain, nausea, diarrhea, and jaundice. The acute form usually appears within the first six months and the chronic form appears later and resembles autoimmune diseases while affecting the skin, mouth, eyes, liver, lungs, joints, gastrointestinal tract, nerves, muscles, and fascia (connective tissue of the skin, eyes, mouth, joints, and organs). Signs and symptoms include rash, jaundice, dyspnea, fatigue, muscle weakness, and decreased range of motion of the joints. GVHD is more likely to occur when the donor is not a close match, is older, or is of a different gender than the recipient.

High-dose corticosteroids (e.g., prednisone) remain the standard first-line treatment of the acute disease [67,68]. Ruxolitinib and abatacept (Table 3) are also used in the management of acute disease. Chronic GVHD is usually treated with long-term immunosuppressive medicines. These include ibrutinib and ruxolitinib after first-line therapy and belumosudil (a ROCK2 blocker) and axatilimab-csfr (CSF-1R blocking antibody) after at least two prior therapies. See Refs. [67,68] for a summary of the clinical trials that led to the approval of these agents.

4. BTK-drug complexes

Acalbrutinib is an amino-pyrazine targeted covalent inhibitor (Fig. 6A) of BTK (IC_{50} value of 3 nM) that is FDA-approved for the treatment of chronic lymphocytic leukemia, small lymphocytic lymphoma, and mantle cell lymphoma. Lin and Andreotti determined the X-ray crystal structure of the mouse BTK-acalabrutinib complex [69]. The kinase domain of the mouse enzyme (residues 401–655) differs from that of the human enzyme by only three residues and we assume that the mouse enzyme is an appropriate model of the human protein. The X-ray structure shows that the amino group attached to the pyrazine moiety hydrogen bonds with the side chain of both the gatekeeper (T474) and the carbonyl backbone of the first hinge residue (E475). A pyrazine nitrogen forms a hydrogen bond with the carbonyl group of the third hinge residue (M477). The drug pyridine nitrogen forms a hydrogen bond with the carbonyl backbone of DFG-D539 (Fig. 7A). The drug makes hydrophobic contact with seven spine residues (RS2/3/4, CS5/6/7/8), two shell residues (Sh2/3), and the KLIFS-3 residue preceding the glycine-rich loop (Table 5) (Fig. 8) [42]. The drug interacts hydrophobically with residues ^{409}GTG^{411} of the G-rich loop, R430 of the β3-strand, M449 of the αC-helix, L460 of the β4-strand, I472 of the β5-strand, residues Y476, M477, G480, C481 of the hinge-linker segment, R525 and N526 of the catalytic loop, S538 (the x of xDFG), DFG-D539, DFG-F540, and L542 of the activation segment. The drug occupies the front pocket, the gate area, the back pocket, and BP-I-B. The enzyme bound to acalabrutinib and the other five drugs in this section assume a BLBplus inactive conformation with αC_{out}, DFG-D_{in}, and a closed activation segment [43]. Acalabrutinib is classified as a type VI inhibitor owing to the covalent nature of the inhibition [41]. See Refs. [70–72] for reports on the use and efficacy of acalabrutinib.

Ibrutinib is a pyrazolo[3,4-*d*] pyrimidine targeted covalent inhibitor (Fig. 6B) of BTK (IC_{50} value of 0.5 nM) that is FDA-approved for the management of the four disorders listed in Table 4 [73]. Bender et al. determined the X-ray crystal structure of the BTK-ibrutinib complex [74] and found that the 4-amino group of the pyrimidine hydrogen bonds with the –OH sidechain of T474 (the gatekeeper residue) and the

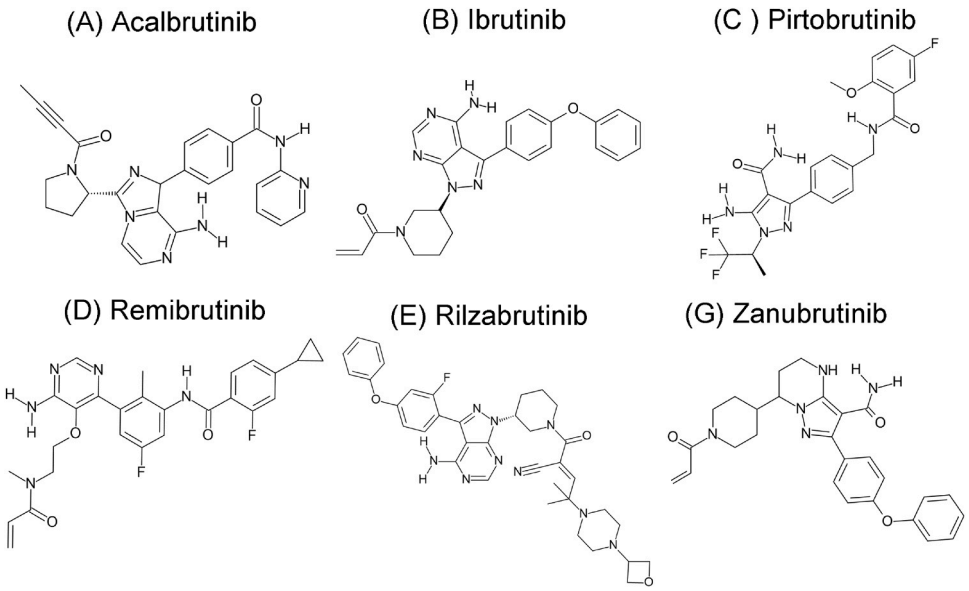

Fig. 6. Structure of FDA-approved BTK inhibitors.

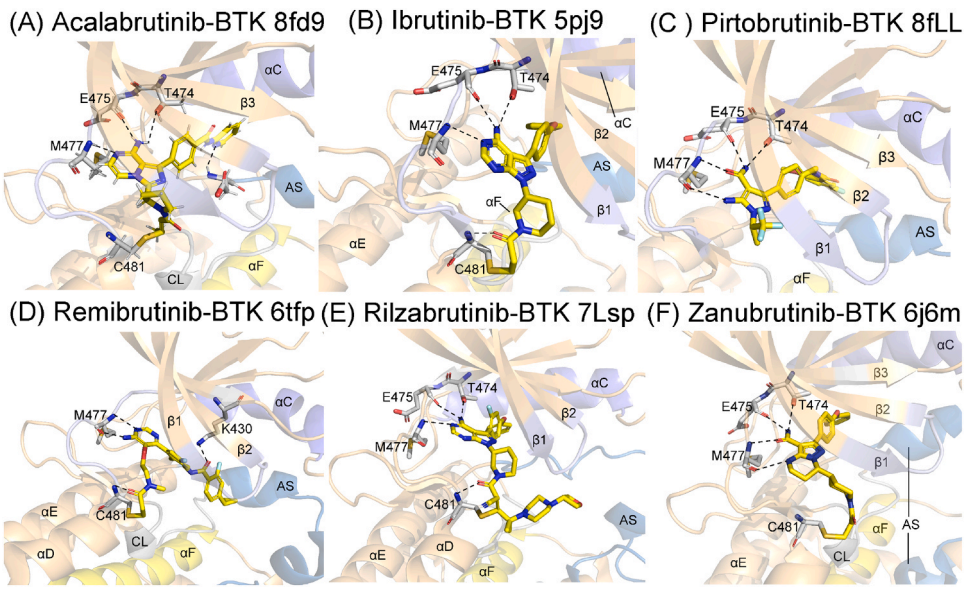

Fig. 7. Structure of BTK-drug complexes. The carbon atoms of the drugs are yellow and those of the enzyme are gray. The dashed lines depict electrostatic bonds. AS, activation segment; CL, catalytic loop.

Table 5
Drug-enzyme hydrophobic (Φ) interactions based upon their common KLIFS residue numbers[a].

	PDB ID ↓	RS1	RS2	RS3	RS4	Sh1	Sh2	Sh3	CS5	CS6	CS7	CS8	KLIFS-3[b]	C[c]/D[d]	KLIFS pockets
KLIFS no. →		68	82	28	38	36	45	43	76	77	11	15	3		
Drug-enzyme ↓															
BTK complexes															
Acalabrutinib-BTK	8fd9		Φ	Φ	Φ		Φ	Φ	Φ	Φ	Φ	Φ	Φ	out/in	F, G, BP-I-B
Ibrutinib-BTK	5p9j		Φ	Φ		Φ	Φ	Φ		Φ	Φ	Φ	Φ	out/in	F, G, B, BP-I-B
Pirtobrutinib-BTK	8fLL		Φ	Φ	Φ	Φ	Φ	Φ		Φ	Φ	Φ	Φ	out/in	F, G, B, BP-I-A/B, BP-II-in
Remibrutinib-BTK	6tfp									Φ	Φ	Φ	Φ	out/in	F, FP-II
Rilzabrutinib-BTK	7L5p		Φ	Φ	Φ	Φ	Φ	Φ		Φ	Φ	Φ	Φ	out/in	F, G, BP-IA/B
Zanubrutinib-BTK	6j6m		Φ	Φ		Φ	Φ	Φ		Φ	Φ	Φ	Φ	out/in	F, G, B, BP-I-B

[a] From klifs.net
[b] KLIFS-3, kinase-ligand interaction fingerprint and structure residue-3
[c] $\alpha C_{in/out}$
[d] DFG-$D_{in/out}$

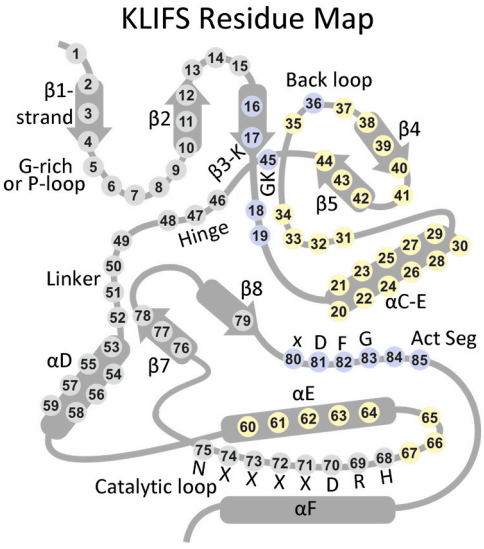

Fig. 8. The location of the KLIFS residues within a generic protein kinase domain. Act Seg, activation segment; GK, gatekeeper. Residues in gray circles are found in the front cleft; blue circles, gate area; yellow circles, back cleft.

carbonyl group of E475 (the first hinge residue). Moreover, the *N*3 pyrimidine hydrogen bonds with the backbone N–H group of M477 (the third hinge residue) and the drug carbonyl moiety hydrogen bonds with the C481 residue within the hinge-linker segment before the αD-helix (Fig. 7B). The acrylamide warhead bonds to the same C481 forming a Michael addition product. The drug makes hydrophobic contact with five spine residues (RS2/3 and CS6/7/8), three shell residues (Sh1/2/3), and the KLIFS-3 residue. The medicinal also interacts hydrophobically with the first residue of the glycine-rich loop (G409), the β3-strand AxK-K430, hinge-linker residues Y476, M477, and C481, the αD-helix N484, S538 (the x of xDFG), DFG-D539, DFG-F540, and L542 of the activation segment. The drug occupies the front pocket, the gate area, the back pocket, and BP-I-B. Owing to the formation of a covalent bond with its drug target, ibrutinib is classified as a type VI inhibitor [41]. See Refs. [6,50,73,75] for a summary of the clinical studies that led to the approval of this compound.

Pirtobrutinib is a pyrazole-4-carboxamide targeted covalent inhibitor (Fig. 6C) of BTK (IC_{50} value of 0.66 nM) that is FDA-approved for the treatment of chronic lymphocytic leukemia, small lymphocytic lymphoma, and mantle cell lymphoma (www.brimr.org/PKI/PKIs.htm). Gomez et al. determined the X-ray crystal structure of the human BTK-pirtobrutinib complex [76] and found that the carboxamide group forms hydrogen bonds with the gatekeeper –OH group (T474), the first hinge residue carbonyl moiety (E475), and the third hinge residue N–H

group (M477). Moreover, a pyrazole nitrogen forms a hydrogen bond with the carbonyl backbone of M477 (Fig. 7C). The drug makes hydrophobic contact with six spine residues (RS2/3/4, CS 6/7/8), the KLIFS-3 residue, G409 of the G-rich loop, AxK-K430, back loop residues V458 and Q459, β4-strand L460, β5-strand I472, the T474 gatekeeper, hinge residue M477, linker residue C481, DFG-D539, DFG-G541, and activation loop residue L542. The medicine occupies the front pocket, the intervening gate area, the back pocket, BP-I-A/B and BP-II-in. BTK bound to the drug exists in the inactive BLBplus conformation and pirtobrutinib is classified as a type I½A reversible inhibitor [41]. This antagonist, which is bound to an inactive enzyme with DFG-D_{in}, is classified as type A (not B) inhibitor because the drug extends into the back pocket.

Remibrutinib is an amino-pyrimidine targeted covalent inhibitor (Fig. 6D) of BTK (K_d value of 0.63 nM) [77] that is FDA-approved for the treatment of chronic spontaneous urticaria (www.brimr.org/PKI/PKIs.htm). Angst et al. determined the X-ray crystal structure of the human BTK-remibrutinib complex and reported that the amino-pyridine hydrogen bonds with M477 (the third hinge residue) and the carbonyl amide of the ligand hydrogen bonds with AxK-K430 [77]. The drug forms a covalent link and a hydrogen bond with C481 of the hinge-linker (Fig. 7D). The drug interacts hydrophobically with three spine residues (CS6/7/8), the KLIFS-3 residue, ^{409}GTGQF^{413} of the G-rich loop, AxK-K430, Y476 and M477 of the hinge, G480 and C481 of the linker, N484 of the αD-helix, HRD-D521 and N526 of the catalytic loop, and S538 (the x of xDFG). The medicinal occupies the front pocket and FP-II. Owing to the formation of a covalent bond with its drug target, remibrutinib is classified as a type VI inhibitor [41]. See Refs. [78,79] for the clinical studies that led to the FDA-approval of pirtobrutinib.

Rilzabrutinib is a pyrazolo[3,4-*d*] pyrimidine reversible targeted covalent inhibitor (Fig. 6E) of BTK (IC_{50} value of 1.3 nM) that is FDA-approved for the management of chronic immune thrombocytopenia [80,81]. Owens et al. determined the X-ray crystal structure of the BTK-rilzabrutinib complex and reported that the pyrazolo-pyrimidine group forms hydrogen bonds with T474 (the gatekeeper residue), E475 (the first hinge residue), and M477 (the third hinge residue) [82]. The carbonyl moiety of the drug forms a hydrogen bond, a covalent bond, and interacts hydrophobically with C481 in the hinge-linker (Fig. 7E). Rilzabrutinib interacts hydrophobically with six spine residues (RS2/3/4, CS6/7/8) and the KLIFS-3 residue. The ligand interacts hydrophobically with ^{409}GTG^{411} of the G-rich loop, I429 and AxK-K430 of the α3-helix, M449 of the αC-helix, V458 of the back loop, L460 of the α4-helix, I472 of the α5-helix, the gatekeeper residue (T474), Y476 of the hinge, L483 and N484 of the αD-helix, R525 of the catalytic loop, S538 (the x of xDFG), DFG-D539, DFG-F540, and L542 of the activation segment. Rilzabrutinib is bound to BTK with an inactive BLBplus conformation. The drug occupies the front pocket, gate area, and BP-IA/B. Owing to the formation of a covalent bond with its drug target, it is classified as a type VI inhibitor [41]. See Ref. [81] for a summary of the clinical trials that led to its approval.

Zanubrutinib is a 4,5,6,7-tetrahydropyrazolo[1,5-*a*] pyrimidine targeted covalent inhibitor (Fig. 6F) of BTK (IC_{50} = 1.5 nM) that is FDA-approved for the treatment of the six disorders listed in Table 4 [83,84]. Guo et al. determined the X-ray crystal structure of the BTK-zanubrutinib complex and found that the carboxamide N–H moiety hydrogen bonds with the –OH sidechain of BTK T474 (the gatekeeper) and the carbonyl group of E475 (the first hinge residue) [85]. Moreover, the pyrimidine N–H moiety hydrogen bonds with the carbonyl backbone of M477 (the third hinge residue) and the carboxamide carbonyl group hydrogen bonds with the N–H portion of this same residue (Fig. 7F). Zanubrutinib interacts hydrophobically with five spine residues (RS2/3 and CS6/7/8), three shell residues (Sh1/2/3), and the KLIFS-3 residue proximal to the glycine-rich loop. The agent also interacts hydrophobically with the β3-strand AxK-K430, T474 (the gatekeeper), hinge-linker residues Y476, M477, G480, C481, plus L483 and N484 of the αD-helix, the catalytic loop residue R525, S538 (the x of xDFG), DFG-D539, DFG-F540, and L542 of the activation segment. The compound forms a covalent bond with the C481 thiol group, the residue of which occurs at the end of the hinge-linker segment. Zanubrutinib occupies the front pocket, the intervening gate area, the back pocket, and BP-I-B. The drug binds to an inactive BLBplus enzyme. Owing to the formation of a covalent bond with its medicinal target, zanubrutinib is classified as a type VI inhibitor [41]. See Ref. [86] for a summary of the clinical trials that led to the approval of this medicine.

5. Epilogue

The term targeted covalent inhibitor (TCI) refers to a compound that binds covalently to a specific molecular target and suppresses its physiological function [87]. Weakly reactive Michael acceptors (most commonly acrylamide derivatives) are the favored warheads that react with various thiols resulting in protein kinase inhibition. In a comprehensive analysis of the protein kinase cysteinome, Liu et al. mapped targetable cysteine residues in and around the ATP-binding pocket [88]. They described six distinct cysteine targets including a cysteine (i) within the Gly-rich loop that occurs in the fibroblast growth factor receptor family (FGFR1/2/3/4), (ii) in the roof of the pocket found in NEK2 and the ribosomal S6 kinase (RSK1/2/3/4) family, (iii) immediately preceding the DFG of ERK2, GSK3β, and the vascular endothelial growth factor receptor family, (iv) in the solvent area found in JAK3 (but not the other JAK family members), (v) in the catalytic loop of Kit (the stem cell factor receptor) and the platelet derived growth factor receptor family, and (vi) after the hinge found in the ErbB1/2/4 epidermal growth factor receptors, Blk of the Src family, and BMX, BTK, ITK, TEC and TXK of the TEC family.

Leproult et al. examined the properties of several covalent protein kinase inhibitors [89]. They suggested that the best approach in the formulation of targeted covalent inhibitors is to capitalize on the reactivity of cysteine thiols in the target enzyme. They identified four distinct cysteine targets contiguous with the protein kinase ATP binding site. One is located after the hinge region of several kinases including C481 of BTK and a second is located on the β2-strand of the ribosomal S6 kinase (RSK1/2/3/4) family. A third group occurs before the DFG motif that occurs in 48 protein kinases and a fourth site is located in the nucleotide binding loop of FGFR1/2/3/4 protein-tyrosine kinases. Baillie classified covalent inhibitors into irreversible (more common) and reversible (less common) inhibitors [90]. Of the five covalent BTK blockers considered in this article, only rilzabrutinib is reversible. Its reactive portion consists of an inverted cyanoacrylamide. Baille noted that the covalent inhibitor approach has gained recognition as a worthwhile element of the medicinal chemist's toolbox and is producing a meaningful impact on the formulation of enzyme antagonists and receptor modulators.

Zhao and Bourne examined possible cysteinyl targets in the protein kinase kinome [91]. They found targets in a nearly a dozen regions in different protein kinases including (i) the glycine-rich loop, (ii) the front pocket, (iii) the gatekeeper residue, (iv) the gatekeeper plus 1, (v) the x residue of xDFG, (vi) DFG plus 2, (vii) the roof of the ATP-binding pocket, (viii) two residues proximal to the catalytic loop HRD, (ix) the activation segment, (x) the extended front pocket, and (xi) remote cysteines. Zhao and Bourne reported that 208 protein kinases have at least one cysteine in the drug binding site [92]. In contrast to cysteine, they suggested that lysine and aspartate are not ideal candidates to undergo a covalent drug interaction given both their conserved character and their abundant distribution [91]. Consequently, investigators have paid more attention to cysteine targets.

Wang et al. expanded the protein kinase cysteinome by using a covalent fragment approach encompassing 47 protein kinases [93]. They recommended that the protein kinase target residues should be non-conserved to increase the selectivity of the inhibitor and to minimize toxicity. Besides its non-conservation, protein cysteine is a favored residue owing to the high nucleophilicity of its thiol sidechain when

compared with all other amino acid side chains. This property makes cysteines amenable to reaction with relatively weak electrophiles thereby decreasing the likelihood of nonspecific reactions. Targeted covalent inhibitors have arisen from the class of drugs to be avoided to those of a favored status. Much of this benefit can be attributed to the clinical effectiveness of ibrutinib [6] (approved by the FDA in 2013) and the other agents reported in this article.

Targeting protein kinases for therapeutic purposes began in earnest in 2001 with the FDA approval of imatinib for the treatment of chronic myelogenous leukemia. The FDA has approved 94 small molecule protein kinase inhibitors for the management of various neoplastic and inflammatory disorders (www.brimr.org/PKI/PKIs.htm). See Ref. [80] for a summary of the molecular weights, number of hydrogen bond donors/acceptors, ligand efficiencies, lipophilic efficiencies, polar surface areas, and solubilities of all 94 FDA-approved small molecule protein kinase inhibitors including the six BTK blockers considered in this review. When the atypical protein kinase inhibitors are added, a total of 99 of these drugs have been approved by the FDA [94]. Ninety-four of these agents are orally bioavailable including the six BTK blockers considered in this article. About three dozen protein kinase drug targets from a family of more than 500 enzymes are being explored in a variety of neoplastic and inflammatory disorders. Most of the FDA-approved drugs (≈ 85) are prescribed for the management of neoplasms including carcinomas, leukemias, and lymphomas; others are used for the treatment of inflammatory and other diseases.

CRediT authorship contribution statement

Robert Roskoski: Writing – review & editing, Writing – original draft, Conceptualization.

Declaration of Competing Interest

The author is unaware of any affiliations, memberships, or financial holdings that might be perceived as affecting the objectivity of this review.

Acknowledgments

I thank Dr. Albert J. Kooistra for providing the template depicted in Fig. 8 and Laura M. Roskoski for providing editorial and bibliographic assistance. I also thank Jasper Martinsek and Josie Rudnicki for their help in preparing the figures and W.S. Sheppard and Pasha Brezina for their help in the analysis of drug properties. The colored figures in this paper were evaluated to ensure that their perception was accurately conveyed to colorblind readers [95].

Data Availability

No data was used for the research described in the article.

References

[1] O.C. Bruton, Agammaglobulinemia, Pediatrics 9 (1952) 722–728.
[2] D. Vetrie, I. Vorechovský, P. Sideras, J. Holland, A. Davies, F. Flinter, L. Hammarström, C. Kinnon, R. Levinsky, M. Bobrow, C.I. Smith, D.R. Bentley, The gene involved in X-linked agammaglobulinaemia is a member of the src family of protein-tyrosine kinases, Nature 362 (1993) 226–233, https://doi.org/10.1038/361226a0.Erratum in: Nature 1993;364:362.
[3] J.D. Thomas, P. Sideras, C.I. Smith, I. Vorechovský, V. Chapman, W.E. Paul, Colocalization of X-linked agammaglobulinemia and X-linked immunodeficiency genes, Science 261 (1993) 355–358, https://doi.org/10.1126/science.8332900.
[4] D.J. Rawlings, D.C. Saffran, S. Tsukada, D.A. Largaespada, J.C. Grimaldi, L. Cohen, R.N. Mohr, J.F. Bazan, M. Howard, N.G. Copeland, et al., Mutation of unique region of Bruton's tyrosine kinase in immunodeficient XID mice, Science 261 (1993) 358–361, https://doi.org/10.1126/science.8332901.
[5] O.C. Bruton, A decade with agammaglobulinemia, J. Pediatr. 60 (1962) 672–676, https://doi.org/10.1016/s0022-3476(62)80092-4.
[6] A. Duminuco, P. De Luca, G. Stanzione, L.A. Caruso, G. Lavenia, S. Scarso, B. Garibaldi, F.E. Palumbo, C. Vetro, G.A. Palumbo, BTK Inhibition in hematology: from CLL/SLL to emerging applications across B-Cell and immune disorders, Biomolecules 16 (2026) 123, https://doi.org/10.3390/biom16010123.
[7] S. Joshi, New insights into SYK targeting in solid tumors, Trends Pharm. Sci. 45 (2024) 904–918, https://doi.org/10.1016/j.tips.2024.08.006.
[8] S. Pal Singh, F. Dammeijer, R.W. Hendriks, Role of Bruton's tyrosine kinase in B cells and malignancies, Mol. Cancer 17 (2018) 57, https://doi.org/10.1186/s12943-018-0779-z.
[9] R. Roskoski Jr, Blockade of mutant RAS oncogenic signaling with a special emphasis on KRAS, Pharm. Res 172 (2021) 105806, https://doi.org/10.1016/j.phrs.2021.105806.
[10] R. Roskoski Jr, RAF protein-serine/threonine kinases: structure and regulation, Biochem Biophys. Res Commun. 399 (2010) 313–317, https://doi.org/10.1016/j.bbrc.2010.07.092.
[11] R. Roskoski Jr, Targeting oncogenic Raf protein-serine/threonine kinases in human cancers, Pharm. Res 135 (2018) 239–258, https://doi.org/10.1016/j.phrs.2018.08.013.
[12] R. Roskoski Jr, MEK1/2 dual-specificity protein kinases: structure and regulation, Biochem Biophys. Res Commun. 417 (2012) 5–10, https://doi.org/10.1016/j.bbrc.2011.11.145.
[13] R. Roskoski Jr, Allosteric MEK1/2 inhibitors including cobimetanib and trametinib in the treatment of cutaneous melanomas, Pharm. Res 117 (2017) 20–31, https://doi.org/10.1016/j.phrs.2016.12.009.
[14] R. Roskoski Jr., ERK1/2 MAP kinases: structure, function, and regulation, Pharm. Res 66 (2012) 105–143, https://doi.org/10.1016/j.phrs.2012.04.005.
[15] R. Roskoski Jr, Targeting ERK1/2 protein-serine/threonine kinases in human cancers, Pharm. Res 142 (2019) 151–168, https://doi.org/10.1016/j.phrs.2019.01.039.
[16] M. Spaargaren, E.A. Beuling, M.L. Rurup, H.P. Meijer, M.D. Klok, S. Middendorp, R.W. Hendriks, S.T. Pals, The B cell antigen receptor controls integrin activity through Btk and PLCγ2, J. Exp. Med 198 (2003) 1539–1550, https://doi.org/10.1084/jem.20011866.
[17] G. Manning, D.B. Whyte, R. Martinez, T. Hunter, S. Sudarsanam, The protein kinase complement of the human genome, Science 298 (2002) 1912–1934, https://doi.org/10.1126/science.1075762.
[18] R. Roskoski Jr, Src protein-tyrosine kinase structure and regulation, Biochem Biophys. Res Commun. 324 (2004) 1155–1164, https://doi.org/10.1016/j.bbrc.2004.09.171.
[19] R. Roskoski Jr, Src protein-tyrosine kinase structure, mechanism, and small molecule inhibitors, Pharm. Res 94 (2015) 9–25, https://doi.org/10.1016/j.phrs.2015.01.003.
[20] Y.C. Shin, A.M. Plummer-Medeiros, A. Mungenast, H.W. Choi, K. TenDyke, X. Zhu, J. Shepard, K. Sanders, N. Zhuang, L. Hu, D. Qian, K. Song, C. Xu, J. Wang, S. B. Poda, M. Liao, Y. Chen, The crystal and cryo-EM structures of PLCγ2 reveal dynamic interdomain recognitions in autoinhibition, Sci. Adv. 10 (2024) eadn6037, https://doi.org/10.1126/sciadv.adn6037.
[21] S.K. Hanks, T. Hunter, Protein kinases 6. The eukaryotic protein kinase superfamily: kinase (catalytic) domain structure and classification, FASEB J. 9 (1995) 576–596.
[22] D.R. Knighton, J.H. Zheng, L.F. Ten Eyck, V.A. Ashford, N.H. Xuong, S.S. Taylor, J. M. Sowadski, Crystal structure of the catalytic subunit of cyclic adenosine monophosphate-dependent protein kinase, Science 253 (1991) 407–414, https://doi.org/10.1126/science.1862342.
[23] D.R. Knighton, J.H. Zheng, L.F. Ten Eyck, N.H. Xuong, S.S. Taylor, J.M. Sowadski, Structure of a peptide inhibitor bound to the catalytic subunit of cyclic adenosine monophosphate-dependent protein kinase, Science 253 (1991) 414–420, https://doi.org/10.1126/science.1862343.
[24] S.S. Taylor, A.P. Kornev, Protein kinases: evolution of dynamic regulatory proteins, Trends Biochem Sci. 36 (2011) 65–77, https://doi.org/10.1016/j.tibs.2010.09.006.
[25] R. Roskoski Jr, A historical overview of protein kinases and their targeted small molecule inhibitors, Pharm. Res 100 (2015) 1–23, https://doi.org/10.1016/j.phrs.2015.07.010.
[26] S.S. Taylor, M.M. Keshwani, J.M. Steichen, A.P. Kornev, Evolution of the eukaryotic protein kinases as dynamic molecular switches, Philos. Trans. R. Soc. Lond. B Biol. Sci. 367 (2012) 2517–2528, https://doi.org/10.1098/rstb.2012.0054.
[27] B. Nolen, S. Taylor, G. Ghosh, Regulation of protein kinases; controlling activity through activation segment conformation, Mol. Cell 15 (2004) 661–675, https://doi.org/10.1016/j.molcel.2004.08.024.
[28] D.J. Rawlings, A.M. Scharenberg, H. Park, M.I. Wahl, S. Lin, R.M. Kato, A. C. Fluckiger, O.N. Witte, J.P. Kinet, Activation of BTK by a phosphorylation mechanism initiated by SRC family kinases, Science 271 (1996) 822–825, https://doi.org/10.1126/science.271.5250.822.
[29] A.P. Kornev, N.M. Haste, S.S. Taylor, L.F. Eyck, Surface comparison of active and inactive protein kinases identifies a conserved activation mechanism, Proc. Natl. Acad. Sci. USA 103 (2006) 17783–17788, https://doi.org/10.1073/pnas.0607656103.
[30] A.P. Kornev, S.S. Taylor, L.F. Ten Eyck, A helix scaffold for the assembly of active protein kinases, Proc. Natl. Acad. Sci. USA 105 (2008) 14377–14382, https://doi.org/10.1073/pnas.0807988105.
[31] R. Roskoski, Jr, Janus kinase (JAK) inhibitors in the treatment of inflammatory and neoplastic diseases, Pharm. Res 111 (2016) 784–803, https://doi.org/10.1016/j.phrs.2016.07.038.
[32] R. Roskoski Jr, Cyclin-dependent protein kinase inhibitors including palbociclib as anticancer drugs, Pharm. Res 111 (2016) 249–275, https://doi.org/10.1016/j.phrs.2016.03.012.

[33] R. Roskoski Jr, Small molecule inhibitors targeting the EGFR/ErbB family of protein-tyrosine kinases in human cancers, Pharm. Res 139 (2019) 395–411, https://doi.org/10.1016/j.phrs.2018.11.014.
[34] R. Roskoski Jr, Anaplastic lymphoma kinase (ALK) inhibitors in the treatment of ALK-driven lung cancers, Pharm. Res 117 (2017) 343–356, https://doi.org/10.1016/j.phrs.2017.01.007.
[35] R. Roskoski, Jr, Vascular endothelial growth factor (VEGF) and VEGF receptor inhibitors in the treatment of renal cell carcinomas, Pharm. Res 120 (2017) 116–132, https://doi.org/10.1016/j.phrs.2017.03.010.
[36] R. Roskoski Jr, ROS1 protein-tyrosine kinase inhibitors in the treatment of ROS1 fusion protein-driven non-small cell lung cancers, Pharm. Res 121 (2017) 202–212, https://doi.org/10.1016/j.phrs.2017.04.022.
[37] R. Roskoski, Jr, A. Sadeghi-Nejad, Role of RET protein-tyrosine kinase inhibitors in the treatment RET-driven thyroid and lung cancers, Pharm. Res 128 (2018) 1–17, https://doi.org/10.1016/j.phrs.2017.12.021.
[38] R. Roskoski Jr, The role of small molecule platelet-derived growth factor receptor (PDGFR) inhibitors in the treatment of neoplastic disorders, Pharm. Res 129 (2018) 65–83, https://doi.org/10.1016/j.phrs.2018.01.021.
[39] R. Roskoski, Jr, The role of small molecule Kit protein-tyrosine kinase inhibitors in the treatment of neoplastic disorders, Pharm. Res 133 (133) (2018) 35–52, https://doi.org/10.1016/j.phrs.2018.04.020.
[40] H.S. Meharena, P. Chang, M.M. Keshwani, K. Oruganty, A.K. Nene, N. Kannan, S. S. Taylor, A.P. Kornev, Deciphering the structural basis of eukaryotic protein kinase regulation, PLoS Biol. 11 (2013) e1001680, https://doi.org/10.1371/journal.pbio.1001680.
[41] R. Roskoski Jr, Classification of small molecule protein kinase inhibitors based upon the structures of their drug-enzyme complexes, Pharm. Res 103 (2016) 26–48, https://doi.org/10.1016/j.phrs.2015.10.021.
[42] O.P. van Linden, A.J. Kooistra, R. Leurs, I.J. de Esch, C. de Graaf, KLIFS: a knowledge-based structural database to navigate kinase-ligand interaction space, J. Med Chem. 57 (2014) 249–277, https://doi.org/10.1021/jm400378w.
[43] V. Modi, R.L. Dunbrack Jr, Kincore: a web resource for structural classification of protein kinases and their inhibitors, Nucleic Acids Res 50 (2022) D654–D664, https://doi.org/10.1093/nar/gkab920.
[44] Q. Wang, E.M. Vogan, L.M. Nocka, C.E. Rosen, J.A. Zorn, S.C. Harrison, J. Kuriyan, Autoinhibition of Bruton's tyrosine kinase (Btk) and activation by soluble inositol hexakisphosphate, Elife 4 (2015) e06074, https://doi.org/10.7554/eLife.06074.
[45] H.C. Kluin-Nelemans, E. Hoster, O. Hermine, J. Walewski, M. Trneny, C.H. Geisler, S. Stilgenbauer, C. Thieblemont, U. Vehling-Kaiser, J.K. Doorduijn, B. Coiffier, R. Forstpointner, H. Tilly, L. Kanz, P. Feugier, M. Szymczyk, M. Hallek, S. Kremers, G. Lepeu, L. Sanhes, J.M. Zijlstra, R. Bouabdallah, P.J. Lugtenburg, M. Macro, M. Pfreundschuh, V. Procházka, F. Di Raimondo, V. Ribrag, M. Uppenkamp, M. André, W. Klapper, W. Hiddemann, M. Unterhalt, M.H. Dreyling, Treatment of older patients with mantle-cell lymphoma, N. Engl. J. Med 367 (2012) 520–531, https://doi.org/10.1056/NEJMoa1200920.
[46] E. Silkenstedt, M. Dreyling, First line therapy in mantle cell lymphoma-the role of BTKi in the initial treatment of transplant-eligible and -ineligible patients, Hematol. Oncol. 43 (2025) e70073, https://doi.org/10.1002/hon.70073.
[47] A.A. Inamdar, A. Goy, N.M. Ayoub, C. Attia, L. Oton, V. Taruvai, M. Costales, Y. T. Lin, A. Pecora, K.S. Suh, Mantle cell lymphoma in the era of precision medicine-diagnosis, biomarkers and therapeutic agents, Oncotarget 7 (2016) 48692–48731, https://doi.org/10.18632/oncotarget.8961.
[48] W.D. Noor, D. Villa, C.Y. Cheah, Approaches to the management of relapsed/refractory mantle cell lymphoma: navigating an increasingly complex therapeutic landscape, Expert Rev. Hematol. 19 (2026) 269–280, https://doi.org/10.1080/17474086.2026.2613730.
[49] G. Fabbri, R. Dalla-Favera, The molecular pathogenesis of chronic lymphocytic leukaemia, Nat. Rev. Cancer 16 (2016) 145–162, https://doi.org/10.1038/nrc.2016.8.
[50] W.G. Wierda, J. Brown, J.S. Abramson, F. Awan, G. Bociek, D. Boyer, M. Cortese, L. Cripe, C. D'Angelo, E. Darnell, R.S. Davis, H. Eradat, N. Esteghamat, L. Fitzgerald, C.D. Fletcher, S. Gaballa, S. Huntington, B. Kahl, M. Kamdar, T. J. Kipps, S. Ma, C.A. Mosse, S. Nakhoda, S.A. Parikh, P. Riedell, A. Schorr, S. Schuster, M. Seshadri, T. Shanafelt, T. Siddiqi, A. Sitlinger, M. Thompson, C. Ujjani, N. Wagner-Johnston, J.A. Woyach, M. Dwyer, H. Sundar, NCCN Guidelines® insights: chronic lymphocytic leukemia/small lymphocytic lymphoma, Version 2.2026, J. Natl. Compr. Canc Netw. 24 (2026) 68–80, https://doi.org/10.6004/jnccn.2026.0012.
[51] R.A. de Claro, K.M. McGinn, N. Verdun, S.L. Lee, H.J. Chiu, H. Saber, M.E. Brower, C.J. Chang, E. Pfuma, B. Habtemariam, J. Bullock, Y. Wang, L. Nie, X.H. Chen, D. R. Lu, A. Al-Hakim, R.C. Kane, E. Kaminskas, R. Justice, A.T. Farrell, R. Pazdur, FDA approval: ibrutinib for patients with previously treated mantle cell lymphoma and previously treated chronic lymphocytic leukemia, Clin. Cancer Res 21 (2015) 3586–3590, https://doi.org/10.1158/1078-0432.CCR-14-2225.
[52] A. Stożek-Tutro, M. Małowicka, K. Janiszewska, P. Kawalec, Systematic review of real-world data on the effectiveness and safety profiles of first-line therapies in chronic lymphocytic leukemia, Crit. Rev. Oncol. Hematol. 221 (2026) 105239, https://doi.org/10.1016/j.critrevonc.2026.105239.
[53] S. Cheng, A. Guo, P. Lu, J. Ma, M. Coleman, Y.L. Wang, Functional characterization of BTK(C481S) mutation that confers ibrutinib resistance: exploration of alternative kinase inhibitors, Leukemia 29 (2015) 895–900, https://doi.org/10.1038/leu.2014.263.
[54] S. Blackmore, S. Elsawa, O. Tavana, The direction of modern therapies in Waldenström macroglobulinaemia, J. Cell Mol. Med 29 (2025) e70987, https://doi.org/10.1111/jcmm.70987.
[55] S.P. Treon, C.K. Tripsas, K. Meid, D. Warren, G. Varma, R. Green, K. V. Argyropoulos, G. Yang, Y. Cao, L. Xu, C.J. Patterson, S. Rodig, J.L. Zehnder, J. C. Aster, N.L. Harris, S. Kanan, I. Ghobrial, J.J. Castillo, J.P. Laubach, Z.R. Hunter, Z. Salman, J. Li, M. Cheng, F. Clow, T. Graef, M.L. Palomba, R.H. Advani, Ibrutinib in previously treated Waldenström's macroglobulinemia, N. Engl. J. Med 372 (2015) 1430–1440, https://doi.org/10.1056/NEJMoa1501548.
[56] S.P. Treon, S. Sarosiek, J.J. Castillo, Diagnosis and management of Waldenstrom's macroglobulinemia, Hematol. Oncol. 43 (2025) e70071, https://doi.org/10.1002/hon.70071.
[57] M.A. Gertz, Waldenström macroglobulinemia: 2025 update on diagnosis, risk stratification, and management, Am. J. Hematol. 100 (2025) 1061–1073, https://doi.org/10.1002/ajh.27666.
[58] E. Goodall, S. Opat, Zanubrutinib in the treatment of Waldenström macroglobulinemia, Future Oncol. 21 (2025) 3151–3158, https://doi.org/10.1080/14796694.2025.2558351.
[59] S. Gaballa, M. Xue, T.I. Totev, D. Pilon, Y. Meng, S. Challagulla, Z. Chen, Y. Wang, K. Yang, Patient medication preferences in follicular lymphoma in the United States: a discrete choice experiment, Post. Med (2026) 1–10, https://doi.org/10.1080/00325481.2026.2641856,Online ahead of print.
[60] F.J. Peñalver, L. Magnano, S. Alonso-Álvarez, A. Jiménez-Ubieto, A. López-Guillermo, J.M. Sancho, Guidelines for diagnosis, treatment, and follow-up of patients with follicular lymphoma-Spanish lymphoma group (GELTAMO) 2025, Cancers 18 (2026) 395, https://doi.org/10.3390/cancers18030395.
[61] N. Akkad, C. Flowers, SOHO state of the art updates and next questions: how should we risk stratify and tailor therapy for patients with high tumor burden follicular lymphoma? A systematic review, Clin. Lymphoma Myeloma Leuk. (2026), https://doi.org/10.1016/j.clml.2025.12.013.
[62] E.A. Martino, S. Caserta, M. Skafi, M.E. Alvaro, A. Bruzzese, N. Amodio, E. Lucia, V. Olivito, C. Labanca, F. Mendicino, E. Vigna, F. Morabito, M. Gentile, Chemotherapy-sparing strategies in follicular lymphoma: emerging targeted and immune-based approaches, Eur. J. Haematol. 116 (2026) 368–379, https://doi.org/10.1111/ejh.70105.
[63] A. Broccoli, M. Del Re, R. Danesi, P.L. Zinzani, Covalent Bruton tyrosine kinase inhibitors across generations: a focus on zanubrutinib, J. Cell Mol. Med 29 (2025) e70170 https:/doi:10.1111/jcmm.70170.
[64] D. Rossi, F. Bertoni, E. Zucca, Marginal-zone lymphomas, N. Engl. J. Med 386 (2022) 568–581, https://doi.org/10.1056/NEJMra2102568.
[65] M.C. Pirosa, A. Stathis, D. Rossi, E. Zucca, SOHO state of the art updates and next questions: treatment options for marginal zone lymphoma, Clin. Lymphoma Myeloma Leuk. 25 (2025) 476–483, https://doi.org/10.1016/j.clml.2025.02.002.
[66] J.P. Alderuccio, A. Noy, The treatment of marginal zone lymphoma, Blood 147 (2026) 115–126, https://doi.org/10.1182/blood.2024028269.
[67] X. Zhang, Y. Ren, R. Huang, X. Wang, X. Zhang, Approved and emerging therapies for glucocorticoid-refractory chronic graft-versus-host disease, Curr. Opin. Immunol. 97 (2025) 102654, https://doi.org/10.1016/j.coi.2025.102654.
[68] L. Steiner, S.A. Klein, S. Kreil, New molecules in the therapy of chronic graft-versus-host disease, Curr. Opin. Hematol. 32 (2025) 314–320, https://doi.org/10.1097/MOH.0000000000000893.
[69] D.Y. Lin, A.H. Andreotti, Structure of BTK kinase domain with the second-generation inhibitors acalabrutinib and tirabrutinib, PLoS One 18 (2023) e0290872, https://doi.org/10.1371/journal.pone.0290872.
[70] T.E. Witzig, D. Inwards, Acalabrutinib for mantle cell lymphoma, Blood 133 (2019) 2570–2574, https://doi.org/10.1182/blood.2019852368.
[71] Y. Khan, S. O'Brien, Acalabrutinib and its use in treatment of chronic lymphocytic leukemia, Future Oncol. 15 (2019) 579–589, https://doi.org/10.2217/fon-2018-0637.
[72] J. Wu, M. Zhang, D. Liu, Acalabrutinib (ACP-196): a selective second-generation BTK inhibitor, J. Hematol. Oncol. 9 (2016) 21, https://doi.org/10.1186/s13045-016-0250-9.
[73] S. Paydas, Management of adverse effects/toxicity of ibrutinib, Crit. Rev. Oncol. Hematol. 136 (2019) 56–63, https://doi.org/10.1016/j.critrevonc.2019.02.001.
[74] A.T. Bender, A. Gardberg, A. Pereira, T. Johnson, Y. Wu, R. Grenningloh, J. Head, F. Morandi, P. Haselmayer, L. Liu-Bujalski, Ability of Bruton's tyrosine kinase inhibitors to sequester Y551 and prevent phosphorylation determines potency for inhibition of Fc Receptor but not B-cell receptor signaling, Mol. Pharm. 91 (2017) 208–219, https://doi.org/10.1124/mol.116.107037.
[75] M.S. Davids, S. Stilgenbauer, C.S. Tam, First-line treatment for CLL in the era of targeted therapy, Blood Cancer J. 16 (2026) 19, https://doi.org/10.1038/s41408-025-01434-2.
[76] E.B. Gomez, K. Ebata, H.S. Randeria, M.S. Rosendahl, E.P. Cedervall, T.H. Morales, L.M. Hanson, N.E. Brown, X. Gong, J. Stephens, W. Wu, I. Lippincott, K.S. Ku, R. A. Walgren, P.B. Abada, J.A. Ballard, C.K. Allerston, B.J. Brandhuber, Preclinical characterization of pirtobrutinib, a highly selective, noncovalent (reversible) BTK inhibitor, Blood 142 (2023) 62–72, https://doi.org/10.1182/blood.2022018674.
[77] D. Angst, F. Gessier, P. Janser, A. Vulpetti, R. Wälchli, C. Beerli, A. Littlewood-Evans, J. Dawson, B. Nuesslein-Hildesheim, G. Wieczorek, S. Gutmann, C. Scheufler, A. Hinniger, A. Zimmerlin, E.G. Funhoff, R. Pulz, B. Cenni, Discovery of LOU064 (remibrutinib), a potent and highly selective covalent inhibitor of Bruton's tyrosine kinase, J. Med Chem. 63 (2020) 5102–5118, https://doi.org/10.1021/acs.jmedchem.9b01916.
[78] R. Roskoski Jr, Properties of FDA-approved small molecule protein kinase inhibitors: a 2024 update, Pharm. Res 200 (2024) 107059, https://doi.org/10.1016/j.phrs.2024.107059.
[79] H.O. Kim, BTK inhibitors and next-generation BTK-targeted therapeutics for B-cell malignancies, Arch. Pharm. Res 48 (2025) 426–449, https://doi.org/10.1007/s12272-025-01546-0.

[80] R. Roskoski Jr, Properties of FDA-approved small molecule protein kinase inhibitors: a 2026 update, Pharm. Res 224 (2026) 108107, https://doi.org/10.1016/j.phrs.2026.108107.
[81] A. Lee, Rilzabrutinib: first approval, Drugs 86 (2026) 385–390, https://doi.org/10.1007/s40265-025-02259-w.
[82] T.D. Owens, K.A. Brameld, E.J. Verner, T. Ton, X. Li, J. Zhu, M.R. Masjedizadeh, J. M. Bradshaw, R.J. Hill, D. Tam, A. Bisconte, E.O. Kim, M. Francesco, Y. Xing, J. Shu, D. Karr, J. LaStant, D. Finkle, N. Loewenstein, H. Haberstock-Debic, M. J. Taylor, P. Nunn, C.L. Langrish, D.M. Goldstein, Discovery of reversible covalent Bruton's tyrosine kinase inhibitors PRN473 and PRN1008 (rilzabrutinib), J. Med Chem. 65 (2022) 5300–5316, https://doi.org/10.1021/acs.jmedchem.1c01170.
[83] M. Das, Zanubrutinib in B-cell malignancies, Lancet Oncol. 20 (2019) e470, https://doi.org/10.1016/S1470-2045(19)30523-6.
[84] Y.Y. Syed, Zanubrutinib: first approval, Drugs 80 (2020) 91–97, https://doi.org/10.1007/s40265-019-01252-4.
[85] Y. Guo, Y. Liu, N. Hu, D. Yu, C. Zhou, G. Shi, B. Zhang, M. Wei, J. Liu, L. Luo, Z. Tang, H. Song, Y. Guo, X. Liu, D. Su, S. Zhang, X. Song, X. Zhou, Y. Hong, S. Chen, Z. Cheng, S. Young, Q. Wei, H. Wang, Q. Wang, L. Lv, F. Wang, H. Xu, H. Sun, H. Xing, N. Li, W. Zhang, Z. Wang, G. Liu, Z. Sun, D. Zhou, W. Li, L. Liu, L. Wang, Z. Wang, Discovery of zanubrutinib (BGB-3111), a novel, potent, and selective covalent inhibitor of Bruton's tyrosine kinase, J. Med Chem. 63 (2019) 7923–7940, https://doi.org/10.1021/acs.jmedchem.9b00687.
[86] A.N. Weaver, A. Jimeno, Zanubrutinib: a new BTK inhibitor for treatment of relapsed/refractory mantle cell lymphoma, Drugs Today (Barc) 56 (2020) 531–539, https://doi.org/10.1358/dot.2020.56.8.3158047.
[87] R. Roskoski Jr, Orally effective FDA-approved protein kinase targeted covalent inhibitors (TCIs), Pharm. Res 165 (2021) 105422, https://doi.org/10.1016/j.phrs.2021.105422.
[88] Q. Liu, Y. Sabnis, Z. Zhao, T. Zhang, S.J. Buhrlage, L.H. Jones, N.S. Gray, Developing irreversible inhibitors of the protein kinase cysteinome, Chem. Biol. 20 (2013) 146–159, https://doi.org/10.1016/j.chembiol.2012.12.006.
[89] E. Leproult, S. Barluenga, D. Moras, J.M. Wurtz, N. Winssinger, Cysteine mapping in conformationally distinct kinase nucleotide binding sites: application to the design of selective covalent inhibitors, J. Med Chem. 54 (2011) 1347–1355, https://doi.org/10.1021/jm101396q.
[90] T.A. Baillie, Targeted covalent inhibitors for drug design, Angew. Chem. Int Ed. 55 (2016) 13408–13421, https://doi.org/10.1002/anie.201601091.
[91] Z. Zhao, P.E. Bourne, Progress with covalent small-molecule kinase inhibitors, Drug Discov. Today 23 (2018) 727–735, https://doi.org/10.1016/j.drudis.2018.01.035.
[92] Z. Zhao, P.E. Bourne, Exploring extended warheads toward developing cysteine-targeted covalent kinase inhibitors, J. Chem. Inf. Model 64 (2024) 9517–9527, https://doi.org/10.1021/acs.jcim.4c00890.
[93] G. Wang, N.J. Seidler, S. Röhm, Y. Pan, X.J. Liang, L. Haarer, B.T. Berger, S. A. Sivashanmugam, V.R. Wydra, M. Forster, S.A. Laufer, A. Chaikuad, M. Gehringer, S. Knapp, Probing the protein kinases' cysteinome by covalent fragments, Angew. Chem. Int Ed. Engl. 64 (2025) e202419736, https://doi.org/10.1002/anie.202419736.
[94] A. Mullard, FDA approves 100th small-molecule kinase inhibitor, Nat. Rev. Drug Discov. 24 (2025) 891–895, https://doi.org/10.1038/d41573-025-00188-7.
[95] R. Roskoski Jr, Guidelines for preparing color figures for everyone including the colorblind, Pharm. Res 119 (2017) 240–241, https://doi.org/10.1016/j.phrs.2017.02.005. Erratum in: Pharmacol Res 139 (2019) 569, https://doi: 10.1016/j.phrs.2018.09.019.